AD-A167 893 A PARAMETRIC STUDY OF ELASTIC RESPONSE OF SUBMARINE-INSTALLED EQUIPMENT S..(U) NAVAL POSTGRADUATE SCHOOL MONTEREY CA G F DECONTO MAR 86 1/2

UNCLASSIFIED F/G 13/10.1 NL

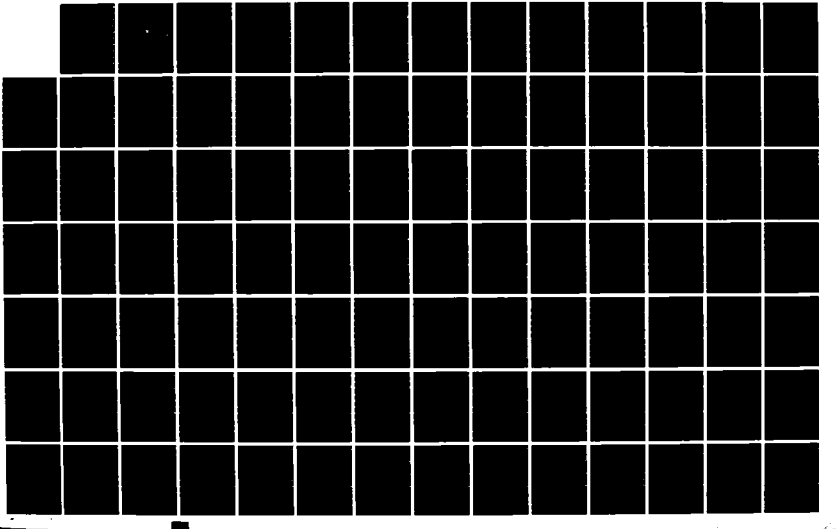

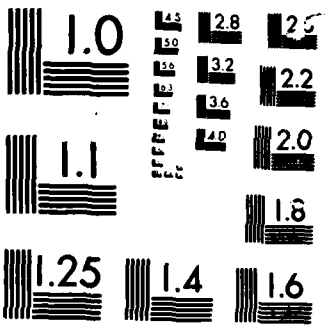

NAVAL POSTGRADUATE SCHOOL
Monterey, California

THESIS

A PARAMETRIC STUDY OF ELASTIC RESPONSE OF SUBMARINE-INSTALLED EQUIPMENT SUBJECTED TO UNDEX SIDE-ON LOADING

by

Gerald Francis DeConto

March 1986

Thesis Advisor: Young S. Shin

Approved for public release; distribution is unlimited.

SECURITY CLASSIFICATION OF THIS PAGE

REPORT DOCUMENTATION PAGE

1a REPORT SECURITY CLASSIFICATION UNCLASSIFIED	1b. RESTRICTIVE MARKINGS
2a. SECURITY CLASSIFICATION AUTHORITY	3 DISTRIBUTION / AVAILABILITY OF REPORT Approved for public release; distribution is unlimited
2b. DECLASSIFICATION / DOWNGRADING SCHEDULE	
4 PERFORMING ORGANIZATION REPORT NUMBER(S)	5. MONITORING ORGANIZATION REPORT NUMBER(S)
6a. NAME OF PERFORMING ORGANIZATION Naval Postgraduate School 6b. OFFICE SYMBOL (If applicable) 69	7a. NAME OF MONITORING ORGANIZATION Naval Postgraduate School
6c. ADDRESS (City, State, and ZIP Code) Monterey, California 93943-5000	7b. ADDRESS (City, State, and ZIP Code) Monterey, California 93943-5000
8a. NAME OF FUNDING / SPONSORING ORGANIZATION 8b. OFFICE SYMBOL (If applicable)	9. PROCUREMENT INSTRUMENT IDENTIFICATION NUMBER
8c. ADDRESS (City, State, and ZIP Code)	10 SOURCE OF FUNDING NUMBERS PROGRAM ELEMENT NO. / PROJECT NO / TASK NO / WORK UNIT ACCESSION NO
11 TITLE (Include Security Classification) A PARAMETRIC STUDY OF ELASTIC RESPONSE OF SUBMARINE-INSTALLED EQUIPMENT SUBJECTED TO UNDEX SIDE-ON LOADING	
12 PERSONAL AUTHOR(S) DeConto, Gerald Francis	
13a TYPE OF REPORT Master's Thesis 13b TIME COVERED FROM _____ TO _____ 14 DATE OF REPORT (Year, Month, Day) 1986, March 15 PAGE COUNT 100	
16 SUPPLEMENTARY NOTATION	
17 COSATI CODES FIELD / GROUP / SUB-GROUP	18 SUBJECT TERMS (Continue on reverse if necessary and identify by block number) ELSHOK, Side-On Loading

19 ABSTRACT (Continue on reverse if necessary and identify by block number)

It is desirable to perform a study of the elastic responses of submarine hulls and internally attached structures to underwater shock loading. In view of the expense and possible involvement of non-shock testable equipment it is not always desirable to perform actual shock tests utilizing real hulls or SSTV's (Submerged Shock Test Vehicles). With the advent of large scale computing power, numerical methods now exist to predict equipment/hull responses. The ELSHOK (ELASTIC SHOCK) computer code is used to perform a parametric study on a submerged shell with an internally attached substructure. Of particular interest is the phenomenon of dynamic amplification or lack of such in the response of this particular substructure and effects on substructure-shell interaction due to varying substructure mass and stiffness subjected to underwater explosion side-on shock loading.

20 DISTRIBUTION / AVAILABILITY OF ABSTRACT ☒ UNCLASSIFIED/UNLIMITED ☐ SAME AS RPT ☐ DTIC USERS	21 ABSTRACT SECURITY CLASSIFICATION UNCLASSIFIED
22a NAME OF RESPONSIBLE INDIVIDUAL Professor Young S. Shin	22b TELEPHONE (Include Area Code) (408) 646-2568 22c OFFICE SYMBOL 69SG

DD FORM 1473, 84 MAR 83 APR edition may be used until exhausted
All other editions are obsolete

SECURITY CLASSIFICATION OF THIS PAGE

Approved for public release; distribution is unlimited

A Parametric Study of Elastic Response of Submarine-Installed Equipment Subjected to UNDEX Side-On Loading

by

Gerald Francis DeConto
Lieutenant, United States Navy
B.S., United States Naval Academy, 1979

Submitted in partial fulfillment of the requirements for the degree of

MASTER OF SCIENCE IN MECHANICAL ENGINEERING

from the

NAVAL POSTGRADUATE SCHOOL
March 1986

Author: Gerald Francis DeConto

Approved by: Young S. Shin, Thesis Advisor

R. E. Newton, Second Reader

Paul J. Marto, Chairman, Department of Mechanical Engineering

John N. Dyer, Dean of Science and Engineering

ABSTRACT

It is desirable to perform a study of the elastic responses of submarine hulls and internally attached structures to underwater shock loading. In view of the expense and possible involvement of non-shock testable equipment it is not always desirable to perform actual shock tests utilizing real hulls or SSTV's (Submerged Shock Test Vehicles). With the advent of large scale computing power, numerical methods now exist to predict equipment/hull responses. The ELSHOK, (ELASTIC SHOCK) computer code is used to perform a parametric study on a submerged shell with an internally attached substructure. Of particular interest is the phenomenon of dynamic amplification or lack of such in the response of this particular substructure and effects on substructure-shell interaction due to varying substructure mass and stiffness subjected to underwater explosion side-on shock loading.

TABLE OF CONTENTS

I. INTRODUCTION 9

A. BACKGROUND 9

B. PURPOSE 10

II. UNDEX SHOCK RESPONSE USING ELSHOK 12

A. ELSHOK PRINCIPLES OF OPERATION 12

B. ORGANIZATION AND IMPLEMENTATION OF ELSHOK . . . 14

1. Phase I--Shell and Fluid Analysis 15

2. Phase II--Structural Analysis of Internal Substructures 17

3. Phase III--Shock Response and Time Integration 18

4. Phase IV--Plotting Velocity Profiles 21

III. MODELS INVOLVED IN THE ANALYSIS 25

A. MODELING WITH FINITE ELEMENT/FINITE DIFFERENCE METHODS 25

B. SUBMERGED SHELL MODELING 25

C. INTERNAL SUBSTRUCTURE MODELING 28

D. SHELL/SUBSTRUCTURE RESPONSE MODELING 31

IV. ANALYSIS 38

A. OBJECTIVES OF ANALYSIS 38

B. ANALYSIS PROCEDURE 39

C. PLOTTING PROCEDURE 43

D. FORCES IN THE SUBSTRUCTURE SUPPORTS 44

V. RESULTS 48

A. SHELL AND SUBSTRUCTURE INTERACTION 48

B. OVERALL SHELL RESPONSES 51

C. FORCES IN THE SUPPORTS 53

VI. CONCLUSIONS 78

LIST OF REFERENCES 81

APPENDIX A: INPUT FILES FOR ELSHOK 83

1. BOSOR4 INPUT DATA FOR ALL CASES 83

2. ACESNID INPUT DATA FOR ALL CASES 86

3. PIFLASH INPUT DATA FOR ALL CASES 87

4. SAP IV INPUT DATA FOR D = 4.2 IN. CASE 88

5. PICRUST INPUT DATA FOR D = 4.2 IN. CASE 89

6. USLOB INPUT DATA 90

7. PUSLOB INPUT DATA 92

APPENDIX B: PROGRAMS USED TO PREPARE AND PLOT VELOCITY PROFILES 94

APPENDIX C: PROGRAM USED TO ESTIMATE AXIAL FORCES IN THE SUPPORT BRACKETS 96

INITIAL DISTRIBUTION LIST 98

LIST OF FIGURES

1. Organization of the ELSHOK Code [Ref. 2] 22

2. Nodal Patterns for Cylindrical Shells 23

3. Pressure-Time History for the Tapered Charge 24

4. Pressure-Time History for the Conventional Charge 24

5. Typical Shell-Substructure Configuration [Ref. 2] 33

6. Ring-Stiffened Cylindrical Shell Model Used in Analysis 34

7. Substructure Model Used in Analysis 35

8. Substructure Model Depicted in SAP IV 36

9. Two-Degrees of Freedom System Model 37

10. Maximum Velocities at Tip of Beam 57

11. Maximum Velocities at Midsection of Beam 58

12. Maximum Velocities at Beam/Bracket Junction 59

13. Maximum Velocities at Shell/Bracket Connection at Frame 18 60

14. Velocity-Time Histories at Beam Tip for D = 4.2 In. 61

15. Velocity-Time Histories at Beam Midsection for D = 4.2 In. 62

16. Velocity-Time Histories at Beam Bracket Junction for D = 4.2 In. 63

17. Velocity-Time Histories at Frame 18 for D = 4.2 In. 64

18. Velocity-Time Histories at Frame 18 for Empty Shell 65

19. Velocity-Time Histories at Frame 18 for Conventional Charge 66

20. Velocity-Time Histories at Frame 18 for Tapered Charge 67

21. Velocity-Time Histories at Midships with Substructure of D = 4.2 In. 68

22. Velocity-Time Histories at Midships for Empty Shell 69

23. Velocity-Time Histories at Frame 9 for Empty Shell 70

24. Velocity-Time Histories at Frame 0 for Empty Shell 71

25. Velocity-Time Histories at Midships for Empty Shell from Conventional Charge 72

26. Velocity-Time Histories at Midships for Empty Shell from Tapered Charge 73

27. Velocity-Time Histories at Frame 18 of Empty Shell from Conventional Charge 74

28. Velocity-Time Histories at Frame 18 of Empty Shell from Tapered Charge 75

29. Velocity-Time Histories at End Plate for Conventional Charge 76

30. Velocity-Time Histories at End Plate for Tapered Charge 77

ACKNOWLEDGEMENT

I would like to thank my thesis advisor, Professor Young Shin, for his patience and guidance, not only in my thesis work but throughout my entire course of instruction at the Naval Postgraduate School. My deep appreciation is extended to Dave Ranlet who instructed me in the use of the ELSHOK code, formulated the idea of this study and was there for technical advice until its completion. I also must express my appreciation and respect for Professor Robert E. Newton for his meticulous review of my work.

I. INTRODUCTION

A. BACKGROUND

A submarine must be able to withstand moderate to severe shock loadings that will result from underwater explosions (UNDEX) it might be subjected to in modern warfare. Conventional and nuclear weaponry deliver devastating forces and no vessel can be expected to survive in the events of near or direct hits. The emphasis on design and testing is in the area of survival of mission critical equipment, machinery and weapons systems of a platform. The ability of a naval vessel to carry out its mission after being subjected to an UNDEX will depend on the survivability of these installations.

The current specifications for building ships and submarines contain the requirements for shock loading to be met by the builder or vendor of shipboard installations and equipment. In general, all critical equipment is required to pass a series of shock tests where testing is practical as outlined in MIL-S-901D [Ref. 1]. This document specifies the shock testing requirements for shipboard machinery, equipment and systems which must resist High Impact (HI) mechanical shock. The purpose of these tests is to determine the suitability of machinery, equipment and

systems for use after exposure to severe shock which may be incurred in wartime. It is not always practical to test equipment due to size and weight. In the case of equipment design, it is not always practical to evaluate an installation prior to final design. Mechanical shock testing of individual equipments may not always indicate how equipment will perform or respond when actually installed. An analysis for a given design is specified for the situations where testing cannot be conducted. It is based on limited and dated testing and observations which are used to specify a shock desigin factor. A static design force is arrived at for various weights of equipment which is used to evaluate the design of support structures of installations. The method is simple to apply but does not always correlate well with actual testing.

Numerical methods have been developed for use in submarine shock response analysis. The computer code ELSHOK (Elastic SHock) developed by Weidlinger Associates for the Office of Naval Research [Ref. 2] is used to conduct this study.

B. PURPOSE

ELSHOK has been developed through a series of controlled tests and has been used to predict equipment responses prior to low level explosive tests on submarines. Although ELSHOK has been validated by extensive testing it is considered

prudent to conduct additional research to gain insight to the sensitivity of the code's predictions when a variety of conditions are applied. The intent of this investigation is to examine the change in the equipment/hull interactions under these conditions. The models used to conduct the parametric study are similar to those used in the mid 1970's in tests conducted by the Office of Naval Research (ONR) [Ref. 3]. The internal structure used was specifically designed to reduce the effects of dynamic amplification for the conditions applied in these tests. The same model geometry was studied here by varying one main dimension to tune the substructure to the natural frequencies of hull to see if this particular internal structure configuration retained this design feature over a range of mass and stiffness variations.

II. UNDEX SHOCK RESPONSE USING ELSHOK

A. ELSHOK PRINCIPLES OF OPERATION

The ELSHOK computer code explained in [Ref. 2] is a suite of computer programs assembled and developed to calculate the submerged shock response of a linearly elastic structure subjected to an underwater shock wave. Specifically, a ring-stiffened shell of revolution of finite length, with or without internal structure, is considered to be immersed, initially at rest, in an infinite acoustic fluid and to be excited by an acoustic shock wave. The shock wave originates from an UNDEX arbitrarily located from the structure and is assumed to propagate as a spherical wave through the medium. This assumption allows incident fluid particle velocities impinging on the wet surface of the immersed structure, the hull of a submarine, to be determined from the incident fluid pressures. ELSHOK contains two possible representations of incident pressure. One uses a known pressure-time profile. This type is of the kind that may be used to describe a tapered charge simulating a nuclear explosion. The other is the empirical decaying exponential put forth by Cole [Ref. 4] for spherical charges of conventional explosives. If the shell contains internal equipment, a substructuring technique

described by Ranlet [Ref. 5] treats the internal equipment response by coupling the free-free modes of the empty ring-stiffened shell and the fixed-base modes of the internal equipment through use of dynamic boundary conditions. Structure-fluid interaction is calculated using the Doubly Asymptotic Approximation (DAA) presented by Geers [Ref. 6]. Normal fluid displacement of the structure-fluid interface is expanded in a series of surface expansion functions which are orthogonal over the entire wet surface of the submerged hull or shell model. The surface expansion functions lead to matrices in which the elements are determined by matching the limits of zero and infinite frequencies of the pressure-velocity relationships. Thus, exact solutions are obtained for the transient problem at early and late times and DAA results in a smooth transition between the two limits. Because DAA calculates the effects of the fluid in the interaction problem through the series of surface expansion functions defined only at the wet surface, the fluid field is in effect uncoupled from the structural field. The fluid effects produced by DAA are simply applied as additional loading in the modal component structural analysis of the shell.

The substructuring technique separately determines the vibration modes of the components that comprise the combined submerged structure of shell and internal substructures.

Equations of motion of the entire structure are obtained by combining interaction forces and moments and enforcing compatibility of deformation at component connection points. This precludes calculations involving the modes and natural frequencies of a system of combined components and also avoids a requirement for a combined system stiffness matrix. The ELSHOK code also handles the case of no substructure in the shell using the same substructuring method.

ELSHOK is particularly suited to the task of a parametric study due to its purely numerical nature and modular organization. Various internal equipment models can be combined repeatedly with the same shell model. Inputs of pressure-time profiles or decaying exponential types are mathematically applied to these numerical models and result in output in the form of velocity-time histories. This transient response analysis takes into account interactions of shell and substructure and eliminates dependency on data derived from actual explosion testing.

B. ORGANIZATION AND IMPLEMENTATION OF ELSHOK

The implementation of ELSHOK is accomplished using a suite of seven major programs. These major components are:

1) BOSOR4 - structural analyzer for shell [Ref. 7]
2) ACESNID - virtual mass processor
3) PIFLASH - shell-fluid processor
4) SAP IV - structural analyzer for substructure [Ref. 8]

5) PICRUST - substructure processor

6) USLOB - time integration processor

7) PUSLOB - plotting processor

Illustrated in Figure 1 are the general relationships between the main components and four phases into which ELSHOK is separated. In any analysis using ELSHOK the shell model and internal structure model must be available or constructed by the user. Development of the models used in this study is discussed later. Once models are arrived at the analysis can be carried out in the four phases by executing each of the seven major programs sequentially in the order listed above.

1. Phase I--Shell and Fluid Analysis

The finite element difference code BOSOR4 is used to analyze the idealized model of the submerged hull or shell. The model must be symmetric about its longitudinal axis and it may contain rings and bulkheads. Circumferential rings can be treated as discrete stiffeners or, if closely spaced, they may be represented in the orthotropic approximation (smeared) [Ref. 9]. An entire main body or full model is used to capture the gross effects of the shell response when calculations are made for circumferential wave numbers N = 0 and 1. These include rigid body translation and whipping of the structure (N = 1) and the torsional modes of the structure (N = 0). Performing the analysis for N = 0 and $\geq$ 2

(breathing mode N = 0) obtains the local shell response. In this analysis wave numbers N = 0, 1, 2, and 3 are used. Figure 2 shows the basic nodal patterns for N = 1-4. ELSHOK requires separate runs of BOSOR4 for each wave N used in the analysis. Each BOSOR4 run determines the in-vacuo free-free modes and corresponding natural frequencies from the dynamic properties and geometry supplied in the model of the shell. If the shell is symmetric about the midpoint of its length and the shock wave impinges on it so as to produce symmetric reponse, only half of the structure need be modeled. Such is the case in this study since the shock wave emanates from an origin located normal to the shell at midships.

ACESNID (Accession to Inertia and Damping) accomplishes the second step of Phase I by calculating the virtual mass array. This provides the late-time contribution of the Doubly Assymptotic Approximation [Ref. 6]. Normal displacements corresponding to the surface expansion functions are applied to the surface of a cavity in the fluid (infinite medium) having the same shape and size as the wet surface of the shell model being investigated. The cavity geometry is obtained from the shell geometry contained in the BOSOR4 output files. Only one run of ACESNID need be performed to encompass all values of N being used and all values of N being used in BOSOR4 must be indicated in ACESNID for compatiblity.

PIFLASH (Prepare Input for Fluid and Shell) accomplishes the last step of Phase I and that is to reorganize the fluid and shell data files from BOSOR4 and ACESNID into a fluid-shell file that is used to solve the response equations. If there are no internal substructures involved in the analysis, then this fluid-shell file is the main input for Phase III and Phase II is not necessary.

2. Phase II--Structural Analysis of Internal Substructures

A finite element model for each internal substructure must be developed. The SAP IV code performs the structural modal analysis on each substructure to be included. The code contains a variety of types of elements that can be used with ELSHOK. Concentrated masses attached to the substructure may also be represented by the methods used in SAP IV. Each substructure requires a separate performance of calculations in which the fixed-base mode shapes and natural frequencies for each are determined. This data is recorded in the "substructure mode file" along with the geometry, stiffness and mass information of the model for future processing.

PICRUST (Prepare Input for Calculating Response of Substructure) rearranges the data from the "substructure mode file" and computes additional information required to solve the response equations. PICRUST also provides for the selection of which modes are to be included from SAP IV and

the specifics of connectivity between the shell and substructure used in the response calculations. Additionally, influence coefficients corresponding to the base motions of the substructure, constraint modes and modal coefficients for calculation of interaction forces with moments between the shell and substructure are determined [Ref. 9]. PICRUST is the last step in Phase III and its results are stored in the substructure file.

3. Phase III--Shock Response and Time Integration

The information required to complete the fluid-structure interaction is supplied as one input file. Therefore, if a substructure is being analyzed in the problem the shell-fluid file from Phase I must be combined with the substructure files produced in Phase II and become the input file for USLOB (Underwater Shock Loading of Bodies) which is ELSHOK's time integration processor. For the case of an empty shell the shell-fluid file is the input for USLOB. Integration is accomplished using a modified Runge-Kutta scheme. The time step and shock wave loading is specified by the user in USLOB. Care must be taken to be sure that the product of the time step chosen and the highest circular structural frequency ω of the modes being used from SAP IV is less than unity. Otherwise, the numerical integration scheme will not converge without changing the time step.

The cases studied in this work used both methods available to represent the incident fluid pressure. A pressure-time history profile shown in Figure 3 was supplied as a typical tapered charge simulation. Nine discrete pressure-time points are entered as input to describe the incident shock wave loading. Tapered charges are used in UNDEX testing to produce the same type of loading resulting from an underwter nuclear detonation. Here the impulse of the shock wave is delivered to the target over a longer period of time compared to the interval over which the impact of a conventional explosive charge is delivered. Both are assumed to emanate from an origin far enough away so as not to include the target in the gas bubble effects. ELSHOK is used for elastic response analysis only and hulls within the immediate vicinity of the gas bubble formed in an UNDEX would most likely have responses well into the plastic response range. Figure 4 shows the pressure-time profile used to represent the incident shock loading of a spherical charge of HBX-1, a conventional explosive, of a weight which would deliver the same impulse over the same period of time as the duration of the tapered charge loading and detonating at the same range from the closest point of the target or standoff. This profile is an empirical exponentially decaying pressure-time history where the initial pressure is the peak incident pressure on the shell due to the charge

weight and standoff. It is seen from Figure 4 that the majority of impulse of the HBX-1 blast is delivered inside the first millisecond. The empirical equation over which USLOB performs integration to obtain the fluid particle velocities is of the form [Ref. 4]:

$$P_I(R,t) = K_1(W^{1/3}/R)^{K_2} \exp(-t/\theta_o) \quad (1)$$

where,

$P_I(R,t)$ = the incident pressure on the hull at range R (ft) from explosive source to point of interest (psi)

K_1 = multiplicative constant for incident pressure

K_2 = spatial decay constant for incident pressure

t = time after arrival of shock wave at point of interest (msec)

W = weight of spherical charge (lb.)

$\theta_o = K_3 W^{1/3}(W^{1/3}/R)^{K_4}$, time constant of exponential decay (msec) (2)

K_3 = multiplicative constant for time constant of exponential decay

K_4 = spatial decay constant for time constant of exponential decay

USLOB creates a generalized velocity file for the shell-substructure and shell-substructure transformation file to be used in the last phase of ELSHOK in producing plotted and printed velocity-time profiles. The transformation file contains information required to describe the motion at the shell-substructure connection points.

4. Phase IV--Plotting Velocity Profiles

PUSLOB (Plots for USLOB) processes the results of the previous three phases so they may be plotted or printed as velocity-time histories. Velocity time-profiles are requested for various locations on the shell and substructure by specifying a call out point in the input files. The call out points are the nodes that are used to describe the models of the shell and substructure in BOSOR4 and SAP IV. Selection of nodes is important because velocities can only be obtained at those locations. The shell velocities may be represented in either a global or local coordinate system. The global is represented by X, Y, Z that locate the positive sense of X toward the bow or forward section of the shell, the positive sense of Y is to port and positive Z is up. The local system is described by u-longitudinal (fwd pos) v-circumferential; w-inward normal from the shell. The substructure is always described by the coordinate system specified in its SAP IV finite element model.

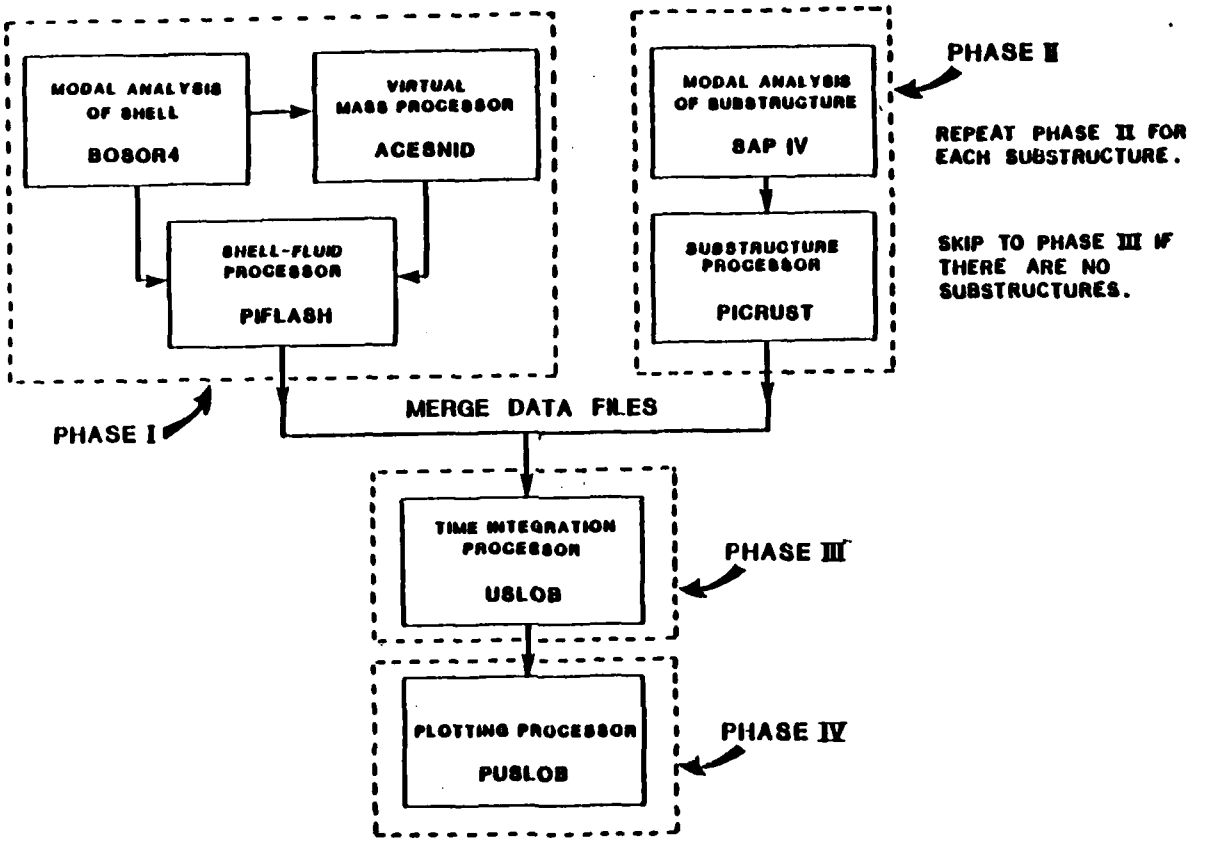

Figure 1. Organization of the ELSHOK Code [Ref. 2]

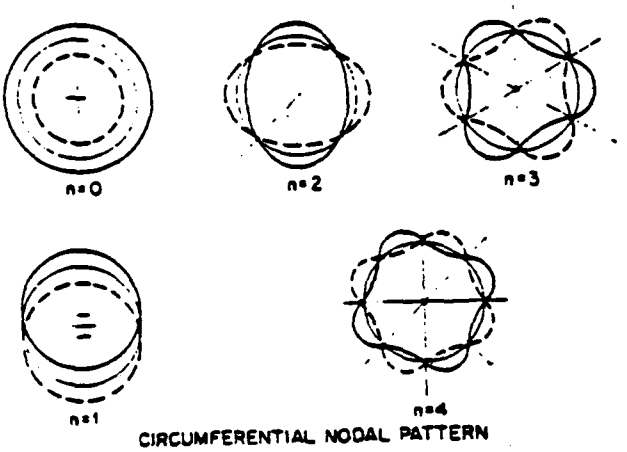

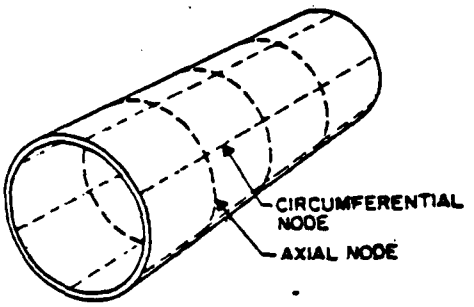

Figure 2. Nodal Patterns for Cylindrical Shells

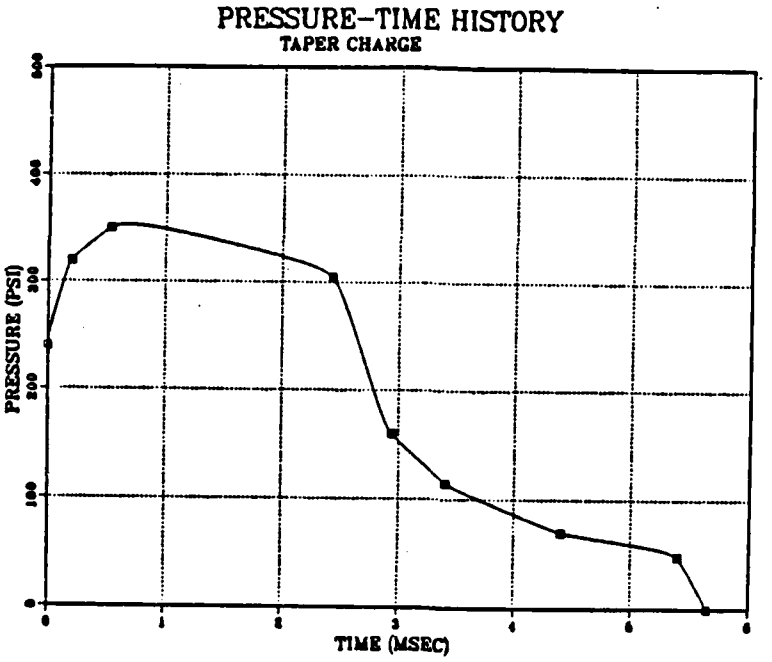

Figure 3. Pressure-Time History for the Tapered Charge

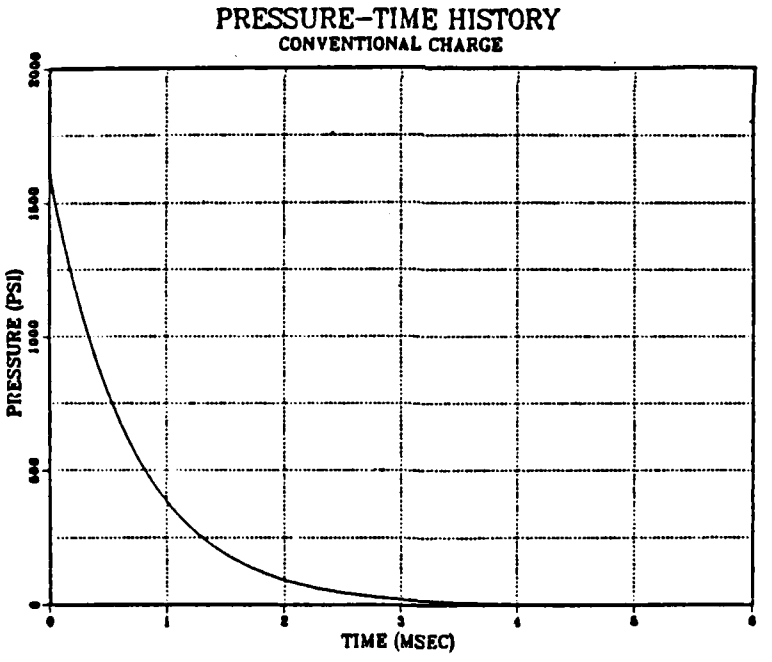

Figure 4. Pressure-Time History for the Conventional Charge

III. MODELS INVOLVED IN THE ANALYSIS

A. MODELING WITH FINITE ELEMENT/FINITE DIFFERENCE METHODS

Finite element/finite difference methods have become powerful tools in engineering with the advent of large scale computing power. These methods are of great use in modeling techniques. Even though the models are much simplified for use in these techniques the results arrived at can be quite accurate or at least adequate for the problems that might be impossible to solve by other methods. Accuracy of the results is closely tied to how well the model represents the actual configuration, so care must be taken when constructing the model. In ELSHOK, the finite difference code BOSOR4 is used to describe the dynamic behavior of underwater hulls by representing them as much simplified models of ring-stiffened shells of revolution. Similarly, the models used to analyze internal substructures are also simplified representations made with the finite element code SAP IV.

B. SUBMERGED SHELL MODELING

Figure 5 is a schematic of the general shell structure and substructure model depicting the notation and convention used to describe the shell global coordinate frame X,Y,Z, shell local coordinate frame u,v,w and the substructure

coordinate frame x,y,z. The z-axis orientation of the local substructure coordinate system is related to the Z-axis of the shell by the angle α_σ where σ represents the substructure. Points are located along the meridian of the shell using the variable s. The angle θ is used to locate circumferentially the desired local shell displacements. One shell model is used in all calculations of this study. Once the symmetric full model was constructed no changes were required to conduct the investigation of varied substructure sizes and types of UNDEX.

The shell or hull that has been modeled for analysis by ELSHOK in this study is similar to an actual structure configured for testing by the Office of Naval Research [Ref. 3]. Figure 6 is a schematic of the representation of the full shell model used. Though its size is much smaller it is also of similar geometry to that of SSTV's (Submerged Shock Test Vehicles) that are used to investigate the underwater shock effects on submarine installed equipment. The model is an idealized submarine hull in that both can be considered as free-free ring-stiffened cylinders with end closures. The shell in this study is in fact a cylinder of revolution made of high strength steel stiffened by six large steel rings plus forty small stringers also of steel. The end plates are aluminum. An internal substructure, also similar to one involved in the testing by ONR is mounted at

midships on the port side of the hull. In BOSOR4 the model is divided into segments of consistent properties contained in each cross section. When the structure is symmetric about the midpoint of its longitudinal axis only one half of the model need be configured. This is accomplished by specifying the appropriate boundary condition at the point of symmetry. In this problem symmetry is employed allowing the shell model to be divided into two segments. Segment one is the aft aluminum end plate and has nine nodes specified on its surface. Node 1/01, node one on segment one, is the center of the end plate. The other nodes move as concentric circles to the outer circumference. Segment two is the cylinder from the end plate to the midships point. Twenty-seven nodes are specified for segment two that are actually bands around its circumference. Node numbers increase from aft to forward such that node 2/27 is the midpoint on the cylinder.

Concentrated masses and substructures internal to the shell must be modeled separately if they contribute significantly to the stiffening of the shell. Therefore, the large rings have been modeled as discrete stiffeners and the internal substructure is modeled separately using SAP IV. If there were no interest in the substructure response it could be modeled as a concentrated mass attached to the shell. There is only one substructure,a doubly overhung

cantilever beam, used in this study and there are no concentrated masses. The smaller stringers do not contribute as significantly to the response of the shell as do the large rings so they are smeared onto the shell to account for their mass [Ref. 9].

The cylindrical section of the shell is a surface of revolution having consistent properties throughout its entire length. This allows information regarding Young's modulus, Poisson's ratio, mass density, thermal expansion coefficients, plating thickness and whether or not rings are smeared to be specified at only one point for the segment in BOSOR4. Similar information is specified for segment one, the end plate. Tables I and II are listings of the natural frequencies and wave numbers for each mode calculated. Twenty-two N = 0 breathing modes, thirty N = 1 rigid body and whipping modes and thirty N = 2,3 modes were retained for analysis. The torsional modes for N = 0 were not retained to eliminate a rotational input at the base of the substructure model. Modal contributions corresponding to N = 2,3 normal, meridional and circumferential displacements were retained for this full model case. Figure 2 shows the basic shapes of the waves on the cylindrical cross section.

C. INTERNAL SUBSTRUCTURE MODELING

In ELSHOK calculations, a substructure model is formulated to determine the modes, masses and natural frequencies

of the internal equipment being analyzed. Phase II of ELSHOK utilizes the SAP IV finite element code to accomplish modeling of submarine-installed equipment. ELSHOK is written in program modules that execute independently and exchange data through the output files. This implementation lends itself well to the type of parametric study conducted in this thesis work. A variety of different internal models may be combined with the same shell model to gain insight on the interaction of the response between the shell and various substructure characteristics. Modeling the substructures in a finite element method more accurately predicts effects of the substructure on the hull to which it is attached than if the model is represented as a concentrated mass. A concentrated mass model would not account for any substructure responses that might become dynamically amplified.

The substructure modeled for this study is a doubly overhung steel beam mounted with steel brackets to the port side of the shell. Connection points are at the two large rings at frames 18 and 27, placing the beam symmetrically about the midships section. Only half of the beam structure requires modeling since symmetry may be employed. Symmetry is indicated in SAP IV by specifying the appropriate boundary condition at the point of symmetry on the model. This is similar to the procedure in BOSOR4. The dimensions

and details of the model are shown in Figure 7. Figure 7 also shows the orientation of the substructure within the shell and to the shockwave. The doubly overhung beam is represented using the three-dimensional beam element model of SAP IV depicted in Figure 8 which shows half the structure with the first mode for D = 4.2 in. superimposed on it. In SAP IV nodes are used to divide the model into separate elements and serve the purpose of call out points for velocity-time histories in Phases III and IV of ELSHOK. Modeling one half of the doubly overhung beam was accomplished using 21 nodes, 4 on the bracket and 17 on the beam half length. The brackets are represented as purely extensional members (a spring with mass) and the introduction of a bending moment at the connection between the beam and bracket is eliminated. This is accomplished by specifying an end release node at node 12 that represents the connection point on the model. The interest in the response of the substructure is limited to the z-direction and restrictions on the degrees of freedom of the model were appropriately specified. This reduces the calculations required and produces responses in the direction of interest.

In order to investigate the response interaction between the shell and substructures of various weights and characteristics the depth D of the beam is changed for each case.

It should be noted that the width of the bracket varies with the depth of the beam by 1.5 x D. Developing the various sized models was accomplished by editing the SAP IV input code to reflect the new cross-sectional areas and moments of inertia for the beam and bracket elements. Other properties remained unchanged.

D. SHELL/SUBSTRUCTURE RESPONSE MODELING

The structural problem of ELSHOK is separated into two parts to avoid calculations involving the modes, natural frequencies and stiffness of a combined system of the shell and substructure. Even though separate modal analysis is carried out on each model in different phases of ELSHOK the responses determined for the shell and substructure are arrived at by coupling the free-free modes of the shell with the fixed-base natural modes of the substructure. In effect the shell and substructure can be approximately represented by a two-degrees of freedom mass-spring model as in Figure 9. Here the mass of the shell is M2 and the stiffness characteristics are K2. The substructure model is represented by M1 and K1. It has been shown for some situations using two single-degree of freedom models can produce nearly the same responses as a two-degrees of freedom model when the mass ratio is very small. This in general does not hold for systems of large mass ratios and is apt to produce marked differences in response between the

two methods if the same stiffness characteristics are used in both [Ref. 10]. ELSHOK results can be viewed with more confidence in predicting component responses because it utilizes the multi-degrees of freedom type model. It is preferred in this study presented due to the large mass ratios that are involved.

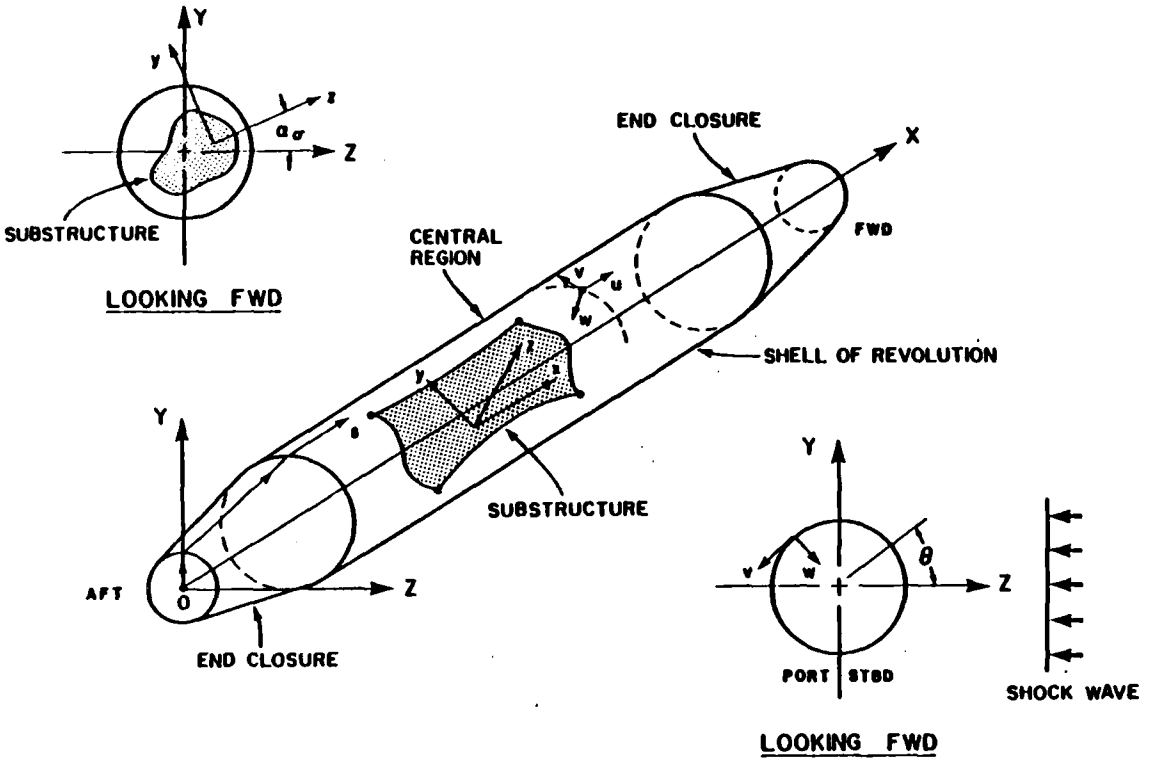

Figure 5. Typical Shell-Substructure Configuration [Ref. 2]

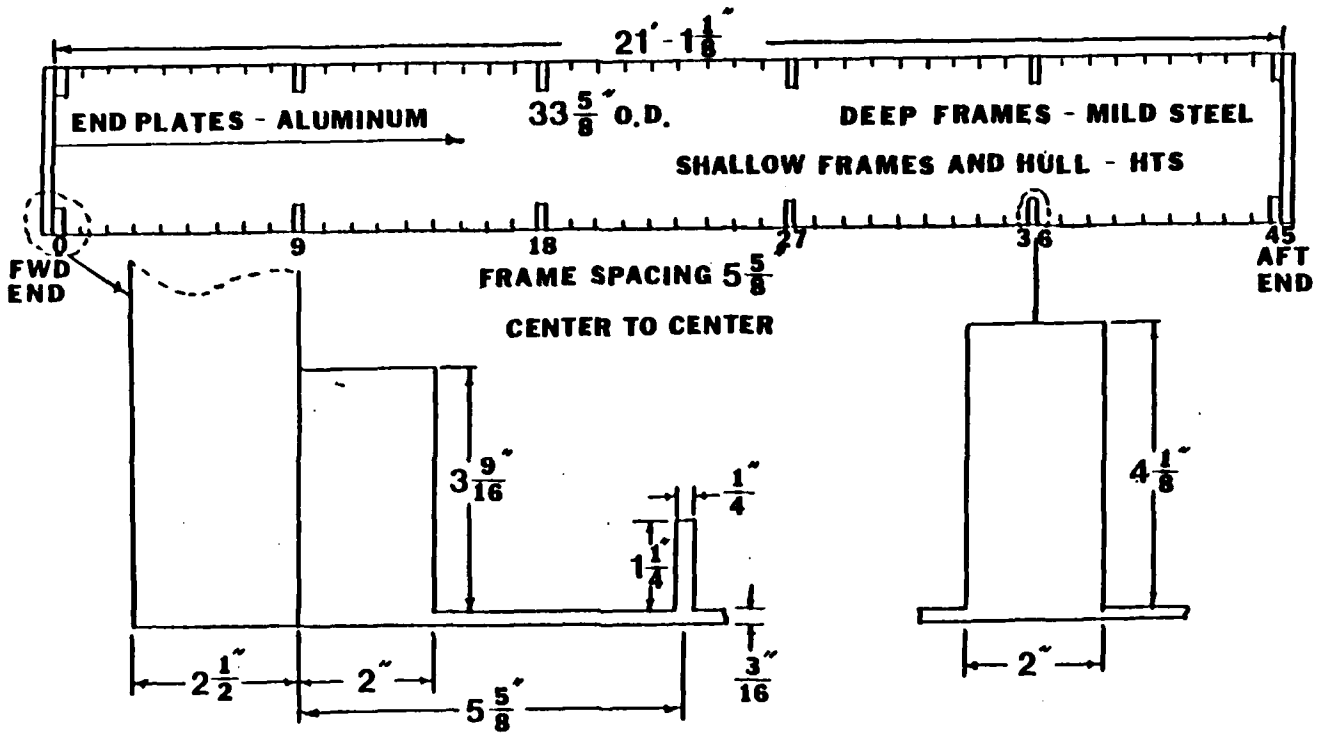

Figure 6. Ring-Stiffened Cylindrical Shell Model Used in Analysis

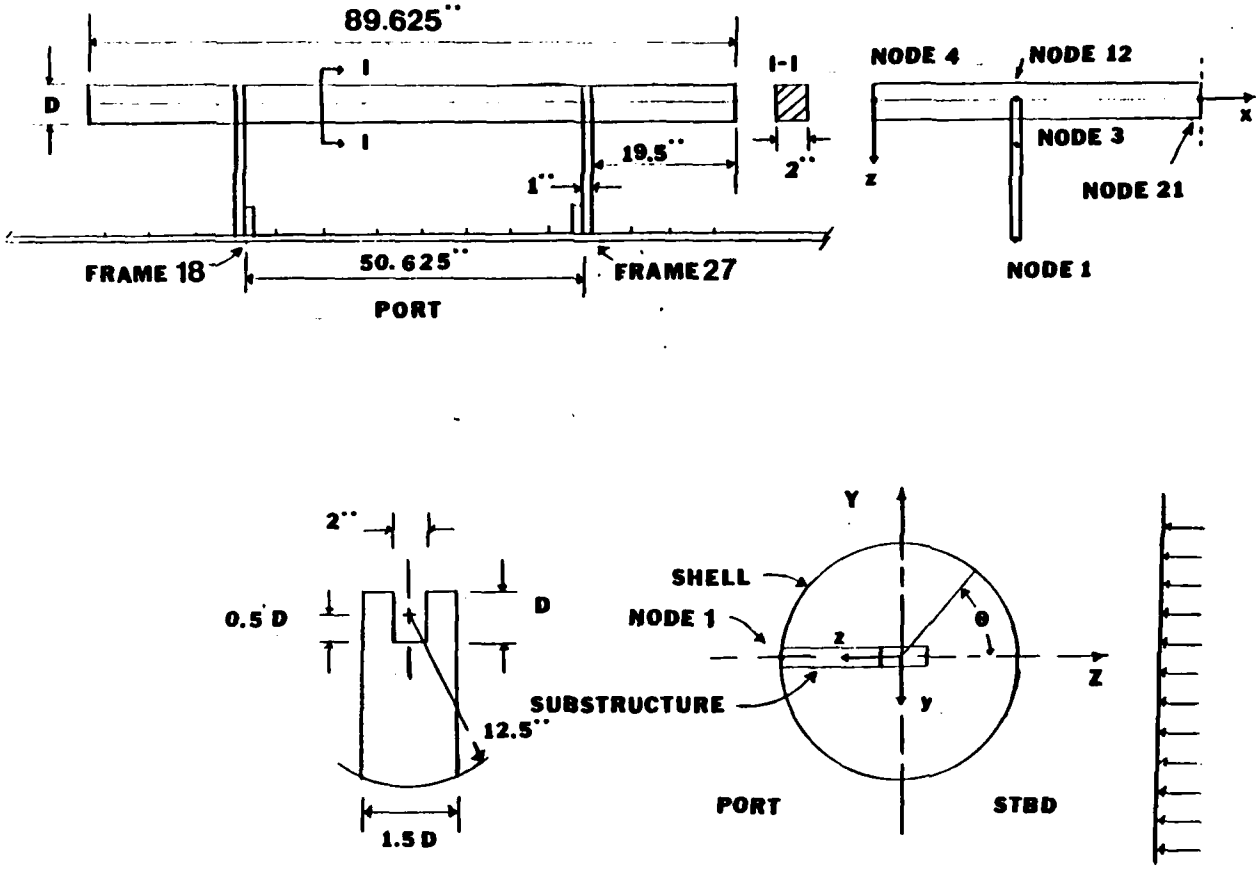

Figure 7. Substructure Model Used in Analysis

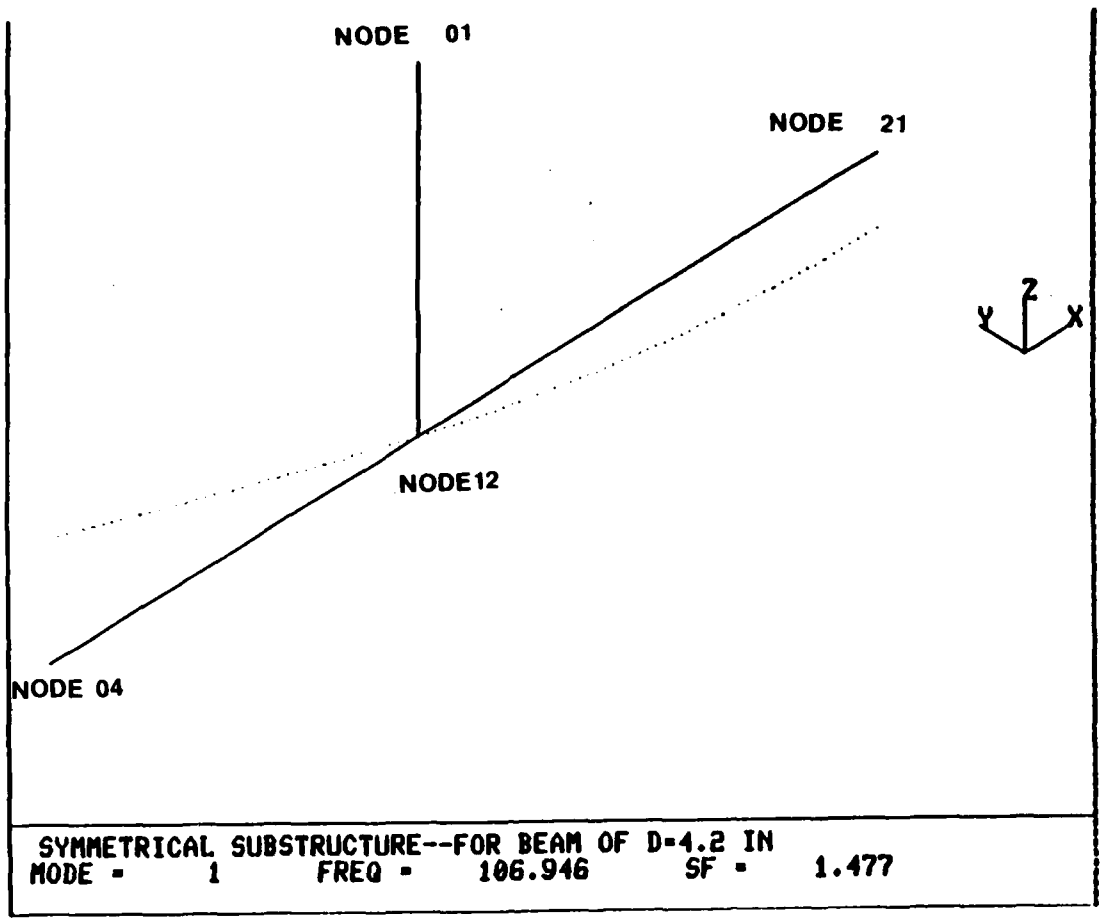

Figure 8. Substructure Model Depicted in SAP IV

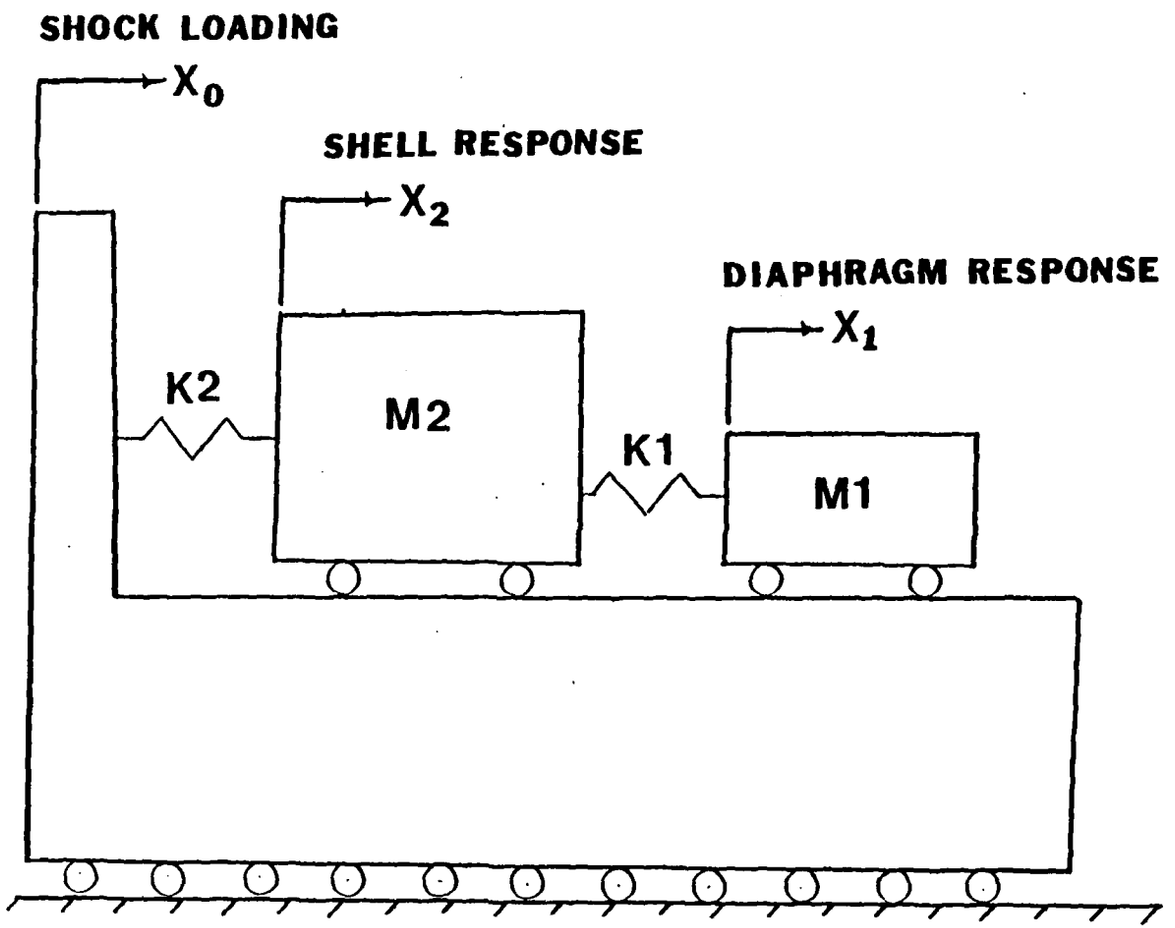

Figure 9. Two-Degrees of Freedom System Model

IV. ANALYSIS

A. OBJECTIVES OF ANALYSIS

The objectives of the analysis procedure are to investigate effects on component responses brought about by varying the mass and stiffness of the internal substructure. More specifically, it is divided into two major and one minor task. First of these is to determine how heavy the internal structure must be before it significantly affects the motion of the shell. Secondly, the dynamic amplification of the responses of the substructure and its effects on the shell are investigated. Lastly, it is of interest to know the magnitude of the forces generated in the support brackets. An integrating scheme is used to determine deflections and thereby estimate the forces.

The shell and substructure are subjected to side-on shock loading from an UNDEX. The UNDEX is represented in two different manners. One is an incident pressure-time history simulating a tapered charge or nuclear detonation and the other is an empirical exponentially decaying incident pressure simulating a spherical conventional charge detonation. The standoff or range from the origin of the UNDEX to the closest point of the target is the same for both the tapered and conventional cases. The weight of the

conventional charge is selected to deliver the same impulse as that of the tapered charge. First, the transient responses of the empty shell are determined for a basis of comparison. Next, responses for a variety of internal structure sizes are calculated for both conventional and tapered charge cases. The results are produced in the form of velocity-time histories and are obtained for points specified on the shell and substructure.

B. ANALYSIS PROCEDURE

The shell natural frequencies and modes for wave numbers N = 0, 1, 2, and 3 are found using the BOSOR4 code. The virtual mass array computed in ACESNID is done including each wave N specified in BOSOR4 for compatibility. In order to simplify the analysis and since the brackets are designed to resist movement out of the horizontal plane, the torsional and rolling modes are eliminated from consideration to prevent a rotational input to the base of the substructure. This is accomplished by setting the variable NTORSN = 0 and omitting any purely rolling or torsional modes for N = 0 from input in the PIFLASH code. All thirty modes for the other values of N are used. This shell model is used throughout the study in combination with each substructure. The BOSOR4 modes deleted and retained are indicated in Tables I and II.

SAP IV was used to determine the fixed-base natural modes and frequencies as D was varied on the substructure

model. The investigation begins with a beam depth D of one inch and increases to twenty inches. It should be noted that twenty inches is nearly physically impossible to fit within the confines of the shell and was computed to investigate the effects of a large mass on the shell. Each SAP IV run produced ten fixed-base natural frequencies corresponding to different mode shapes of the doubly overhung beam. Table III contains frequencies computed for the cases D = 1.0, 4.2 and 9.0 in. Not all the modes determined in each case were used in the follow-on calculations because some of the high frequencies would not allow convergence of the integrating scheme used without changing the time step. All modes having frequencies of 3979 Hz and greater were not used in the analysis. These higher modes do not contribute significantly enough to warrant varying the time step to remain within the convergence limits.

Results from each SAP IV run require processing by the PICRUST code for preparation to merge the shell and substructure data files with the fluid data files. The configuration of each substructure installation along with the modes to be used in Phase III calculations are specified. The substructure z-axis is related to the shell coordinate system by the angle α_σ shown in Figure 5. The meridional locations of the attachment points are also specified here. Each case investigated placed the

substructure attached to the port side or an angle of 180° from the shell Z-axis orientation (exactly one half the distance between the top and bottom). The brackets connect to the rings at frames 18 and 27 placing the substructure evenly about the midships section of the shell or node 2/27. Each case D is subjected to two types of UNDEX representations having origins at 70 ft. (840 in.) from the shell abeam the starboard side at midships. The origin also is located in the shell's Z-X plane. After PICRUST prepares the shell/substructure-fluid data the time integration of the incident pressures experienced by the shell surface is performed to determine velocities.

The USLOB code models the type of UNDEX by differently representing the incident pressures. The tapered charge pressure-time history is represented by inputting discrete pressure-time points that describe it. The conventional spherical charge is represented by equation (1) and specifying the appropriate constants for the type of explosive used. The weight of the charge specifies the size of the explosion and its resultant impulse and incident pressure on the shell. In determining a charge weight that would deliver the same impulse as the tapered charge pressure-time history equations from Cole [Ref. 4] and constants describing HBX-1 were used. Describing the impulse of unit area of the shock wave front up to a time t after its arrival at the shell wet surface by:

$$I(t) = \int_0^t P(t)\,dt \tag{3}$$

where: $P(t) = P_o \exp(t/\theta_o)$ (4)

Then integrating equation (2) over the time after arrival of the shock wave results in:

$$I(t) = P_o\theta_o[1 - \exp(-t/\theta_o)] \tag{5}$$

Substituting equation (2) for θ_o and P_o where,

$$P_o = K_1(W^{1/3}/R)^{K_2} \tag{6}$$

into equation (5) then setting it equal to the area under the curve in Figure 3 the charge weight arrived at through iteration is 352 lbm of HBX-1. The constants for HBX-1 are determined from data recorded in feet and msec. This required K_1 and K_2 to be adjusted to represent the empirical relationships in inches and seconds in order to be consistent with the units used in this application of ELSHOK.

The standoff and lateral placement of the origin of the UNDEX is specified in USLOB along with the duration of integration and the time step to be used. A time duration of 10 msec and a step of $3\text{x}10^{-5}$ sec was used to capture the peak response in each case. Also no effects due to surface

cutoff or reflection of shock waves were considered. This situation represents a deep submerged test simulation where bulk cavition due to the surface doesn't occur and there is no bottom bounce or surface cutoff effects.

C. PLOTTING PROCEDURE

Plotting of velocity profiles is accomplished by PUSLOB in the last phase of ELSHOK. Each profile is a record of the velocity history for a single node specified on the shell or substructure. The plot is limited to two angular locations of the shell nodes and velocities are expressed in in/sec due to the units used in this study. The version of ELSHOK available at the Naval Postgraduate School is installed on the VAX/VMS system and plots were produced on Tektronix devices. In order to aid in comparing the velocities of different nodes the data files used to create the PUSLOB plots were processed using program PLOTCONV. Program PLOTCONV rearranges the data files and converts the units of velocity from in/sec to ft/sec. This facilitates the use of plotting routines EASYPLOT or DISSPLA available on the school's IBM system and expresses the plots in the customary units of the shock community: velocity in ft/sec, time in msec. Program FISH1 is a program developed for use with the DISSPLA plotting routine. Copies of programs PLOTCONV and FISH1 are found in Appendix B.

D. FORCES IN THE SUBSTRUCTURE SUPPORTS

Since ELSHOK produces results in velocity-time histories, force calculations require some post processing. Forces generated in the support brackets would be mainly due to extension and compression because the bracket design resists motion out of the horizontal plane. Due to this and to simplify the analysis, inertia of the brackets is neglected in the force calculations, though their mass is included in the shock response calculations of ELSHOK. Program FORCES found in Appendix C was used to convert the velocity histories to deflections using a Simpson's one-third integrating scheme. Uniaxial forces estimated are based on $F = \epsilon EA$ where ϵ is the estimated deflection of the bracket divided by the length between the connection points of bracket at the ring and beam junction. E is the modulus of elasticity of steel and A is the cross section area of the bracket, 1.5 x D.

TABLE I

MODES AND FREQUENCIES OF SHELL MODEL FOR WAVE NOS. N = 0,1

Mode	N	Freq. (Hz)	N	Freq. (Hz)	Mode	N	Freq. (Hz)	N	Freq. (Hz)
* 1	0	8.344E-04	1	2.340E-05	16	0	1.904E+03	1	1.729E+03
* 2	0	3.128E+02	1	6.444E+01	17	0	1.910E+03	1	1.734E+03
3	0	2.252E+02	1	2.762E+02	18	0	1.913E+03	1	1.772E+03
4	0	4.619E+02	1	6.274E+02	19	0	1.916E+03	1	1.831E+03
* 5	0	6.141E+02	1	7.299E+02	20	0	1.918E+03	1	1.841E+03
6	0	7.561E+02	1	8.351E+02	21	0	1.920E+03	1	1.850E+03
7	0	1.038E+03	1	1.038E+03	22	0	1.921E+03	1	1.855E+03
* 8	0	1.131E+03	1	1.013E+03	23	0	1.923E+03	1	1.871E+03
* 9	0	1.318E+03	1	1.156E+03	24	0	1.924E+03	1	1.881E+03
*10	0	1.570E+03	1	1.185E+03	25	0	1.925E+03	1	1.888E+03
*11	0	1.659E+03	1	1.315E+03	26	0	1.927E+03	1	1.895E+03
*12	0	1.670E+03	1	1.435E+03	27	0	1.927E+03	1	1.892E+03
13	0	1.803E+03	1	1.526E+03	28	0	1.929E+03	1	1.897E+03
14	0	1.861E+03	1	1.645E+03	29	0	1.980E+03	1	1.898E+03
15	0	1.892E+03	1	1.673E+03	30	0	1.991E+03	1	2.213E+03

(* Deleted Modes for N = 0)

TABLE II

MODES AND FREQUENCIES OF SHELL MODEL FOR WAVE NOS. N = 2,3

Mode	N	Freq. (Hz)	N	Freq. (Hz)	Mode	N	Freq. (Hz)	N	Freq. (Hz)
1	2	3.259E+02	3	3.987E+02	16	2	1.608E+03	3	1.549E+03
2	2	3.369E+02	3	4.204E+02	17	2	1.661E+03	3	1.614E+03
3	2	3.676E+02	3	4.344E+02	18	2	1.689E+03	3	1.635E+03
4	2	5.166E+02	3	7.319E+02	19	2	1.728E+03	3	1.657E+03
5	2	6.103E+02	3	7.418E+02	20	2	1.756E+03	3	1.676E+03
6	2	6.694E+02	3	9.642E+02	21	2	1.774E+03	3	1.688E+03
7	2	9.617E+02	3	1.065E+03	22	2	1.790E+03	3	1.696E+03
8	2	1.016E+03	3	1.093E+03	23	2	1.802E+03	3	1.748E+03
9	2	1.186E+03	3	1.147E+03	24	2	1.809E+03	3	1.748E+03
10	2	1.237E+03	3	1.318E+03	25	2	1.814E+03	3	1.792E+03
11	2	1.318E+03	3	1.339E+03	26	2	1.913E+03	3	2.419E+03
12	2	1.358E+03	3	1.360E+03	27	2	1.993E+03	3	2.444E+03
13	2	1.474E+03	3	1.371E+03	28	2	2.211E+03	3	2.780E+03
14	2	1.492E+03	3	1.428E+03	29	2	2.524E+03	3	3.191E+03
15	2	1.571E+03	3	1.518E+03	30	2	2.760E+03	3	3.570E+03

TABLE III

SUBSTRUCTURE NATURAL FREQUENCIES

Mode	Frequency (Hz)		
	D = 1.0 in.	D = 4.2 in.	D = 9.0 in.
1	25.46	106.9	228.7
2	81.63	330.5	616.3
3	337.4	1354.0	1728.0
4	463.0	1421.0	3032.0
5	966.4	2700.0	4982.0
6	1206.0	4167.0	6552.0
7	1802.0	5475.0	8951.0
8	2151.0	6728.0	9957.0
9	2680.0	8380.0	12430.0
10	3281.0	9939.0	17810.0

V. RESULTS

Numerous cases were explored in this parametric study in which the beam depth D varied over the range of one to twenty inches. ELSHOK generated a large amount of information about each case. The most significant results have been summarized in tabular and plotted forms which contain information on cases subjected to the tapered charge and the conventional charge UNDEX simulations. SAP IV predicted frequencies and modes for the tapered charge case with beam depth D = 4.0 in. that compared very closely with the ONR model previously tested. This provides a certain amount of confidence in the SAP IV model used throughout this investigation.

A. SHELL AND SUBSTRUCTURE INTERACTION

Even though the variation of substructure sizes included the cases resulting near the 600 Hz secondary frequency that was expected to induce dynamic amplification in the original ONR model there is no such response over the entire range of cases investigated. The case for D = 4.2 in. conventional charge resulted in a peak of velocities at the tip and midsection of the beam as shown in Figure 10 and Figure 11. However, this is not a resonant condition. This slight amplification can be traced back to shell modes 1, 2, 3 for

N = 2 and mode 1 for N = 3. Tables IV and V summarize the range of results for both charge types and, when viewed with Figures 12 and 13, there is some indication of transfer of energy between the substructures and the hull, but not much. There seems to be no significant interaction between the beam and shell. The basic shape of the velocity-time histories at the beam tip, midsection and junction remain nearly the same throughout the range of D studied. The only effects seem to be the decrease of beam and bracket maximum velocities as the weight of the beam is increased. The complete velocity profiles for the beam bracket and connection points for the D = 4.2 in. cases are shown in Figures 14 through 17. This size was selected for comparison because it did demonstrate slightly higher overall velocities on the beam and also falls nearly into mid-range of the cases if D = 15.0 and 20.0 in. are regarded as unreasonable models due to their size. These two cases were looked at simply to check the effect of the large mass they would represent on the hull. Noting Figure 13 that shows the maximum velocities of the bracket connection points, the rings at frames 18 and 27, it is seen that the variation in peak responses is only slight over the range of D = 4.0-10.0 in. for the tapered charge case. This corresponds to substructure to shell mass ratios of .07644-.19875. The empty shell velocity at this point is 10.48 ft/sec and its

highest maximum velocity occurs when D = 7.0 in. which is 11.88 ft/sec corresponding to a mass ratio of .13638. The conventional charge empty shell velocity at this point was 32.14 ft/sec and this was the maximum velocity recorded on frames 18 and 27 of the conventional cases.

The velocity-time histories of the beam and bracket for the cases D = 2.0-10.0 in. for both charge types are very similar to the D = 4.2 in. cases shown in Figures 14 through 16. At D = 1.0 in. the response was very oscillatory and produced the largest maximum velocity for the conventional charge at the beam tip. This could be due to the large impulse combined with the smallest mass ratio of .01874. The other cases simply show overall decreases in velocities but retained the basic shape of the velocity-time histories. Comparing the empty shell to the shell with substructure velocity-time histories at the midsection of the shell and frame 18 demonstrates what little contribution the substructures' responses made in the shell response. In Figures 17 through 20 the shape of the velocity-time history profiles for these points can be seen to be mostly unchanged by the presence of the substructure. This was true for all cases, conventional and tapered, and increasing the weight of the substructure served mostly to reduce the velocity at the connection point.

Comparing the frequencies of the shell model from Table II with the first five natural frequencies of the substruc-

ture models there are very few matched frequencies at and below 600 Hz which are the range expected to excite the first two modes of the substructure. The frequencies for the cases listed in Table III show how quickly they increase to magnitudes where their contributions to response is minimal. Any modes of the substructure being excited by the base input at the connection points of the brackets and shell did not result in a dynamically amplified response. Each increment of substructure size produces a set of fixed base frequencies of larger magnitude than the previous set. If the natural frequency is equal to:

$$\omega_n = \sqrt{K/M_e} \tag{7}$$

where K = stiffness and M_e = effective mass then the stiffness must be increasing more rapidly than the mass of each structure to produce the higher frequencies.

B. OVERALL SHELL RESPONSES

The shell response overall seems to exhibit some of the expected modes for the circumferential waves used in the calculations with the exception of the purely torsional modes that were deleted early on. First looking at the velocity-time histories in Figures 21 through 24 the extreme difference in velocities produced by the two types of charges is apparent. As expected, the conventional charge

produces larger velocities in each case. These velocities are in the athwart ship direction, positive sense to port, at call out points on the midships station and the three frames where the discrete rings are located. The velocity-time histories due to the conventional charge illustrate how the velocities propagate from the midships station to the end plates. Looking at the peak velocities the shell can be seen to be bending about the midships station while the entire shell translates in the direction of the shock wave. These modes can be seen in the velocity profiles for conventional and tapered charge cases where the midships peak velocity is less than those for the two rings located at frames 9 and 18. Looking at Figures 22 and 25 shows that the velocities at the midships station for the conventional case on the port and starboard sides are of opposite signs at about time equal to 1.0-2.0 msec. This illustrates a higher order circumferential wave of N = 2. Figures 25 and 26 show the velocity profiles at the top of the shell in the athwart ship direction. In each case run the top and bottom velocity profiles were exactly matched indicating the symmetric response to the shock loading in the translational and whipping modes. Figures 27 and 28 illustrate the slight lag in the velocities on the port side. As a rule the conventional starboard side velocities at ring frames were always higher than the port. This is due to the short

duration of shock front of the conventional charge. Alternately, the tapered charge caused slightly higher peak velocities on the port side but also lagged the peak responses on the stbd side. This shows how the tapered charge allows the port side to exhibit more response to the exciting forces.

The end plate velocities are shown in Figures 29 and 30. The end plate in Figure 29 can be seen to bulge in and out at the center for the conventional case and in Figure 30 the tapered case shows the same response. The ring at frame zero tends to hold the outer circumference of the end plate in place as shown by the lower velocities experienced at the outer edge. These velocity-time histories are indicative of breathing modes of the shell.

C. FORCES IN THE SUPPORTS

The axial forces were estimated for the D = 4.2 in. model subjected to both the conventional and tapered charges. In both cases the forces fluctuate between compressive and tensile as indicated by the changes in sign in the results in Appendix C. The maximum force estimated occurred in the conventional case. It was a compressive force of about 103 kips or a stress of about 16 psi. The maximum tensile force experienced by the support bracket for this case was estimated at approximately 75 kips. The tapered charge case produced much lower force estimates.

The maximum was tensile and occurred at about 1.7 msec whereas the conventional maximum force occurred at about .3 msec. The maximum estimated tensile and compressive forces for the tapered charge case are 25 kips and 23 kips, respectively.

TABLE IV

SUMMARY OF RESULTS--TAPERED CHARGE

D(in)	F1(Hz)	F2(Hz)	MAXIMUM VELOCITIES (FPS)				M1/M2
			TIP(04)	MID(21)	JCN(12)	2/21(180°)	
1	25.46	81.63	27.92	19.76	10.96	10.32	.01874
2	50.92	162.2	24.58	21.79	11.39	10.19	.0377
3	76.38	240.6	22.10	19.14	11.02	10.11	.05696
4	101.8	315.9	21.18	18.85	11.94	11.37	.07644
4.2	106.9	330.5	20.71	18.52	11.97	11.53	.0765
5	127.3	387.1	18.98	17.21	11.98	11.76	.09602
6	152.8	453.4	17.49	15.87	11.89	11.72	.11615
7	178.2	514.0	15.69	14.33	12.12	11.88	.13638
8	203.7	568.7	13.72	12.70	11.83	11.69	.15685
9	228.7	616.3	12.05	11.76	11.43	11.24	.1775
10	254.6	659.6	12.04	11.75	11.11	10.99	.19875
15	381.9	798.5	11.16	11.17	10.74	10.81	.3071
20	509.2	863.3	10.79	10.75	10.68	10.37	.4219

(Shell mass M2 = 3420.0 lbm,

Empty shell V(2/21) = 10.48 FPS)

TABLE V

SUMMARY OF RESULTS--CONVENTIONAL CHARGES

D(in)	F1(Hz)	F2(Hz)	MAXIMUM VELOCITIES (FPS)				M1/M2
			TIP(04)	MID(21)	JCN(12)	2/21(180°)	
1	25.46	81.63	77.21	43.93	33.97	31.75	.01874
2	50.92	162.2	55.66	41.32	31.97	29.81	.0377
3	76.38	240.6	51.59	39.90	33.44	27.85	.05696
4	101.8	315.9	58.51	48.48	30.77	28.02	.07644
4.2	106.9	330.5	59.16	48.91	29.87	27.83	.0765
5	127.3	387.1	58.04	48.76	26.56	26.43	.09602
6	152.8	453.4	54.42	47.06	24.18	23.45	.11615
7	178.2	514.0	49.22	43.05	24.48	21.78	.13638
8	203.7	568.7	43.33	38.35	25.06	23.02	.15685
9	228.7	616.3	37.78	33.81	34.55	23.33	.1775
10	254.6	659.6	32.35	29.65	23.48	22.90	.19875
15	381.9	798.5	20.91	20.34	19.65	19.69	.3071
20	509.2	863.3	17.44	17.47	17.12	16.95	.4219

(Shell mass M2 = 3420.0 lbm,

Empty shell V(2/21) = 34.14 FPS)

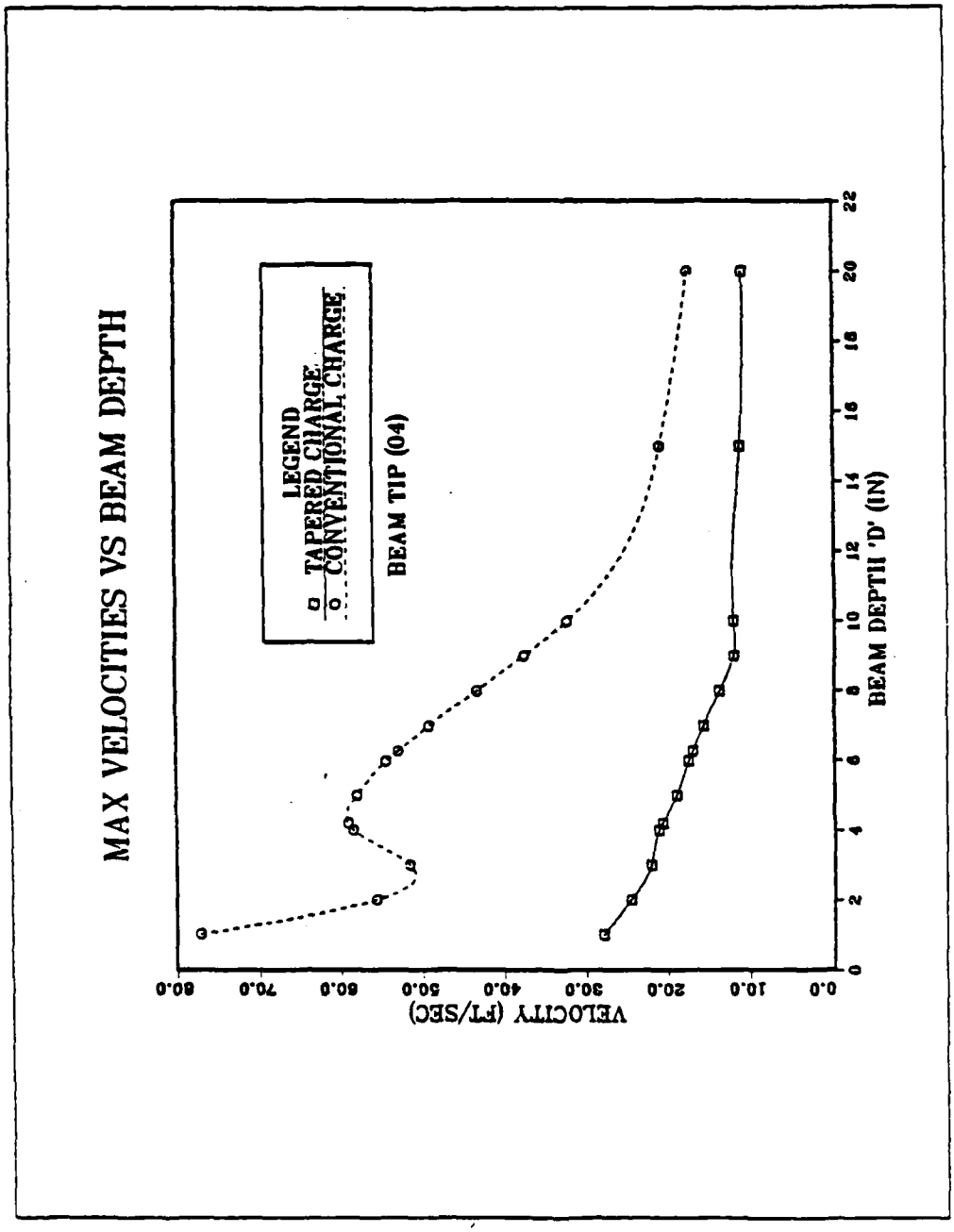

Figure 10. Maximum Velocities at Tip of Beam

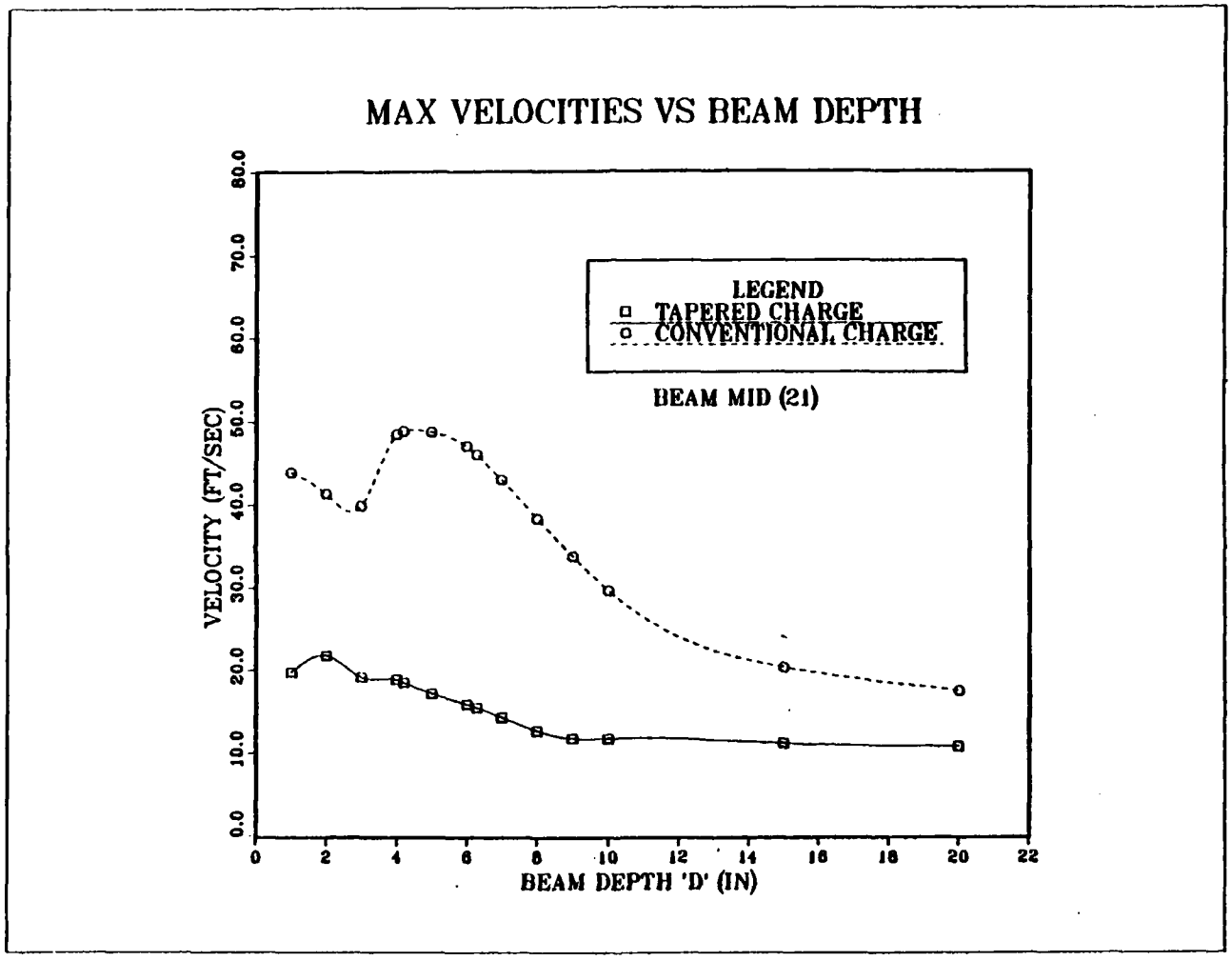

Figure 11. Maximum Velocities at Midsection of Beam

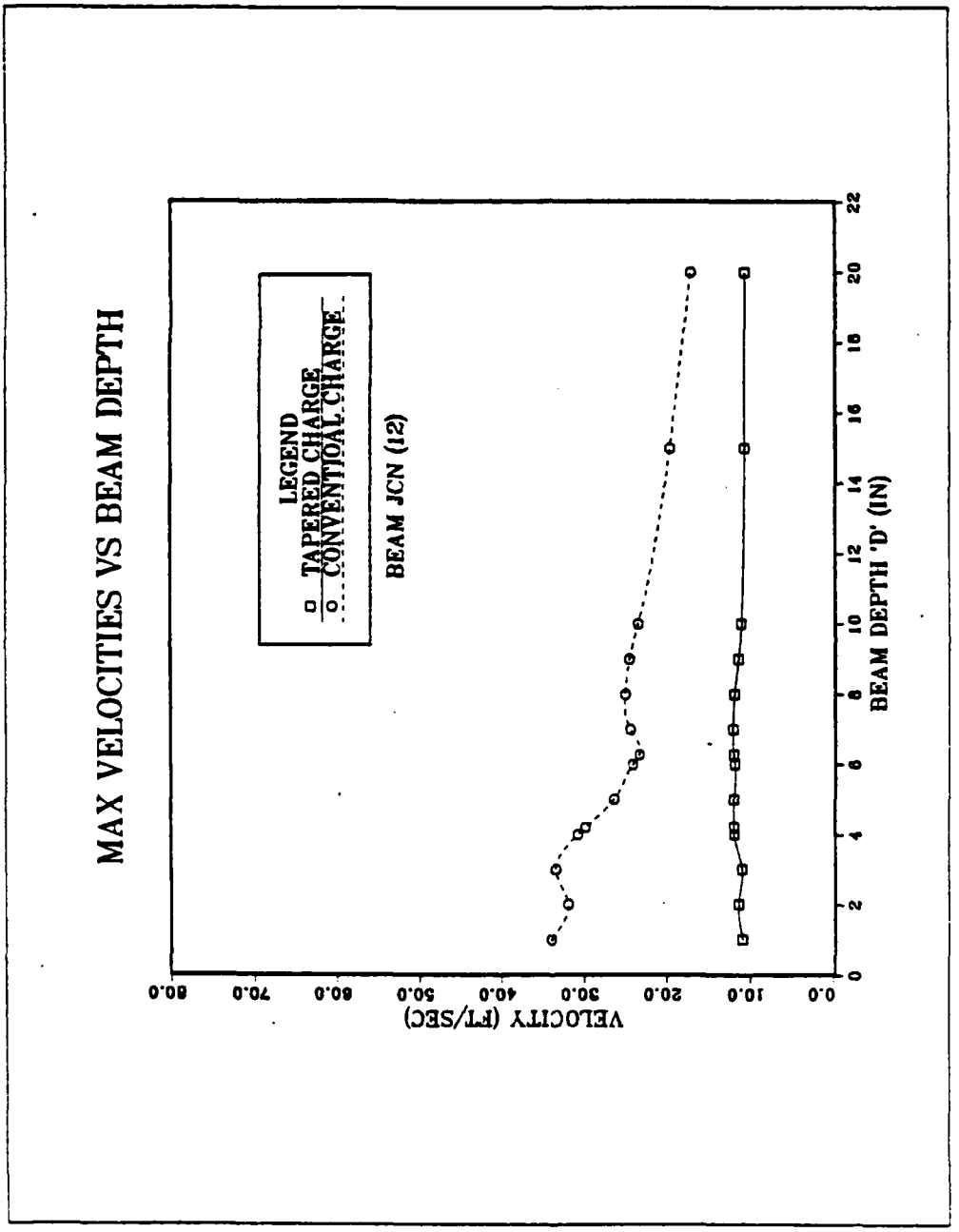

Figure 12. Maximum Velocities at Beam/Bracket Junction

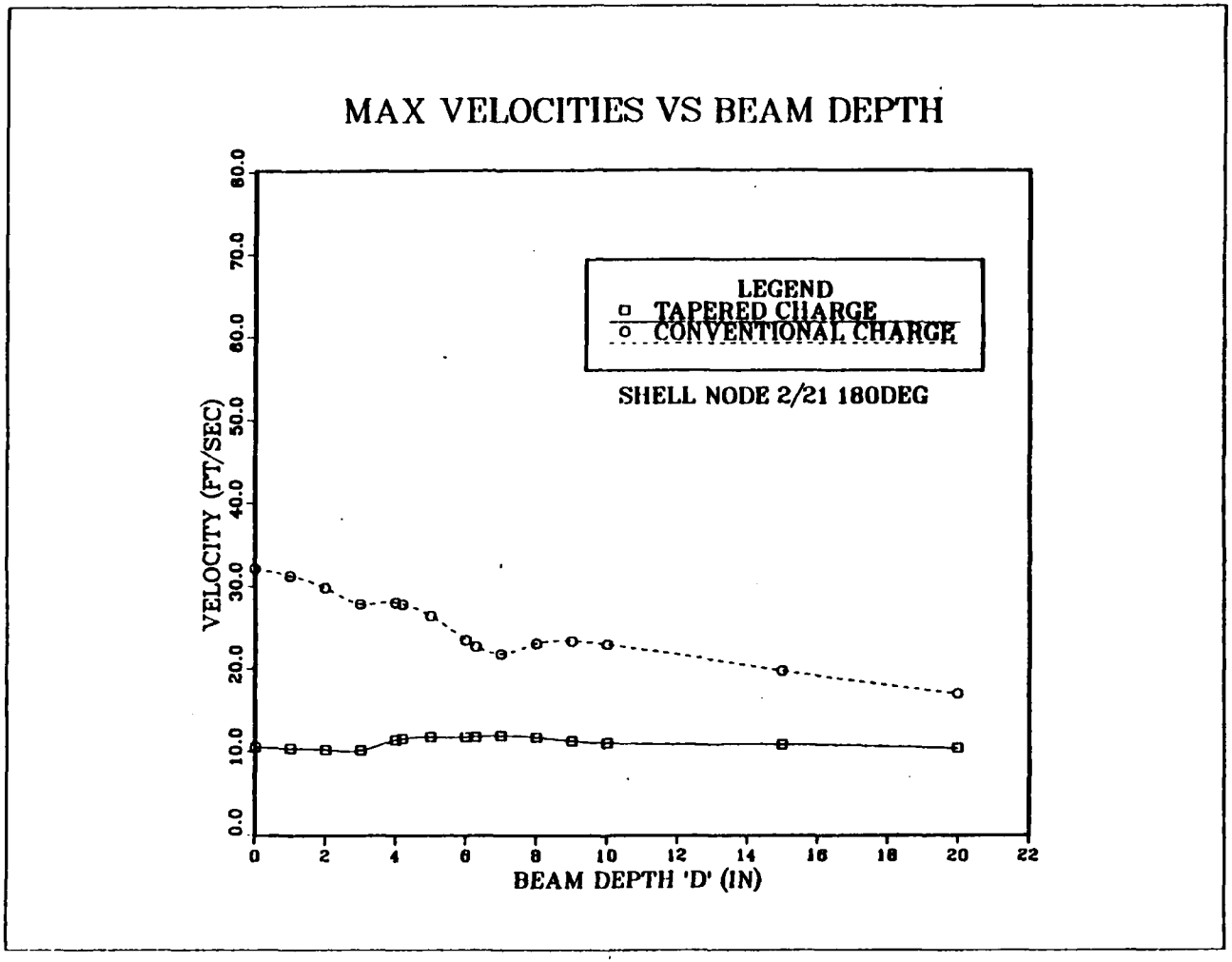

Figure 13. Maximum Velocities at Shell/Bracket Connection at Frame 18

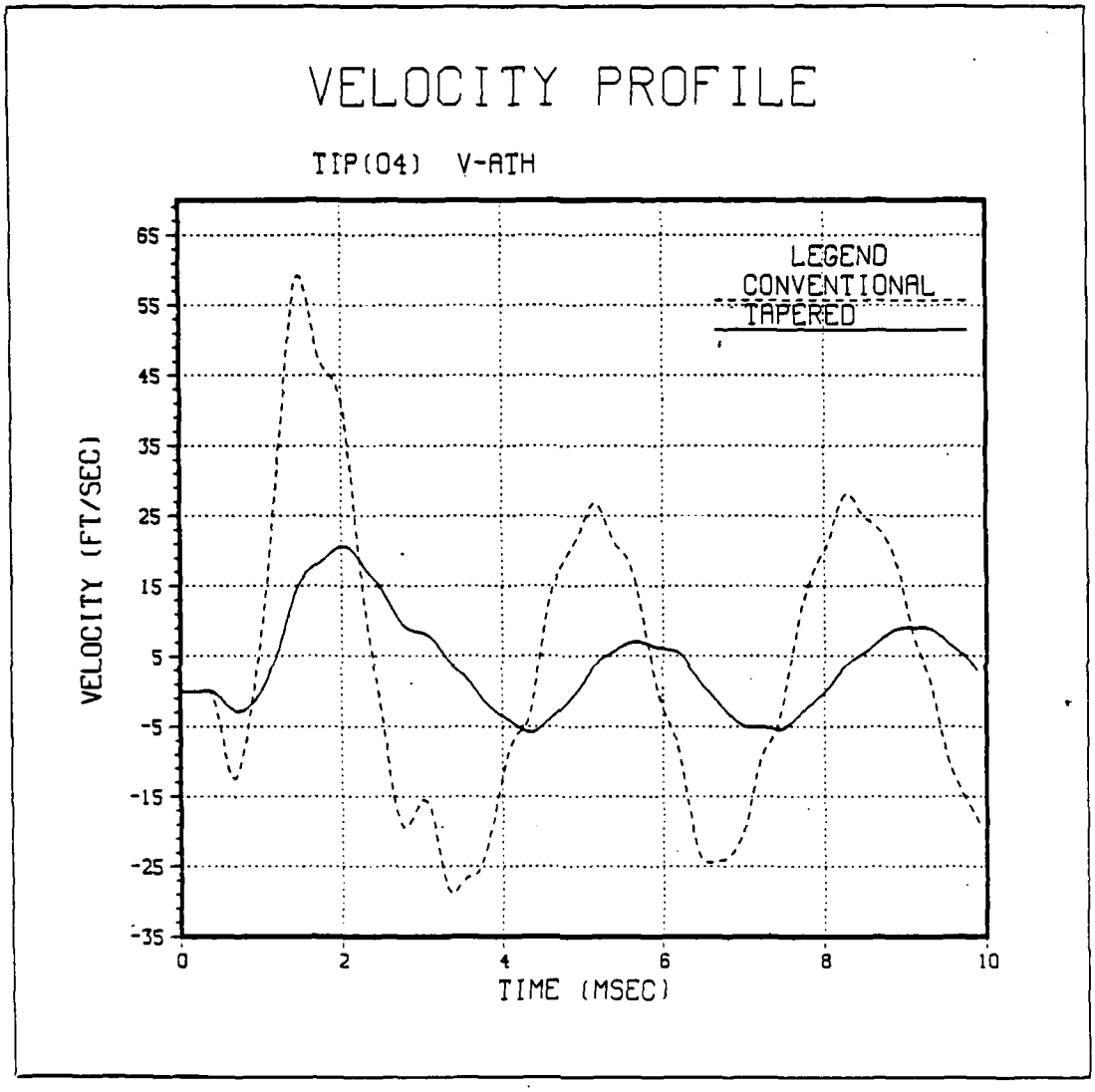

Figure 14. Velocity-Time Histories at Beam Tip for D = 4.2 In.

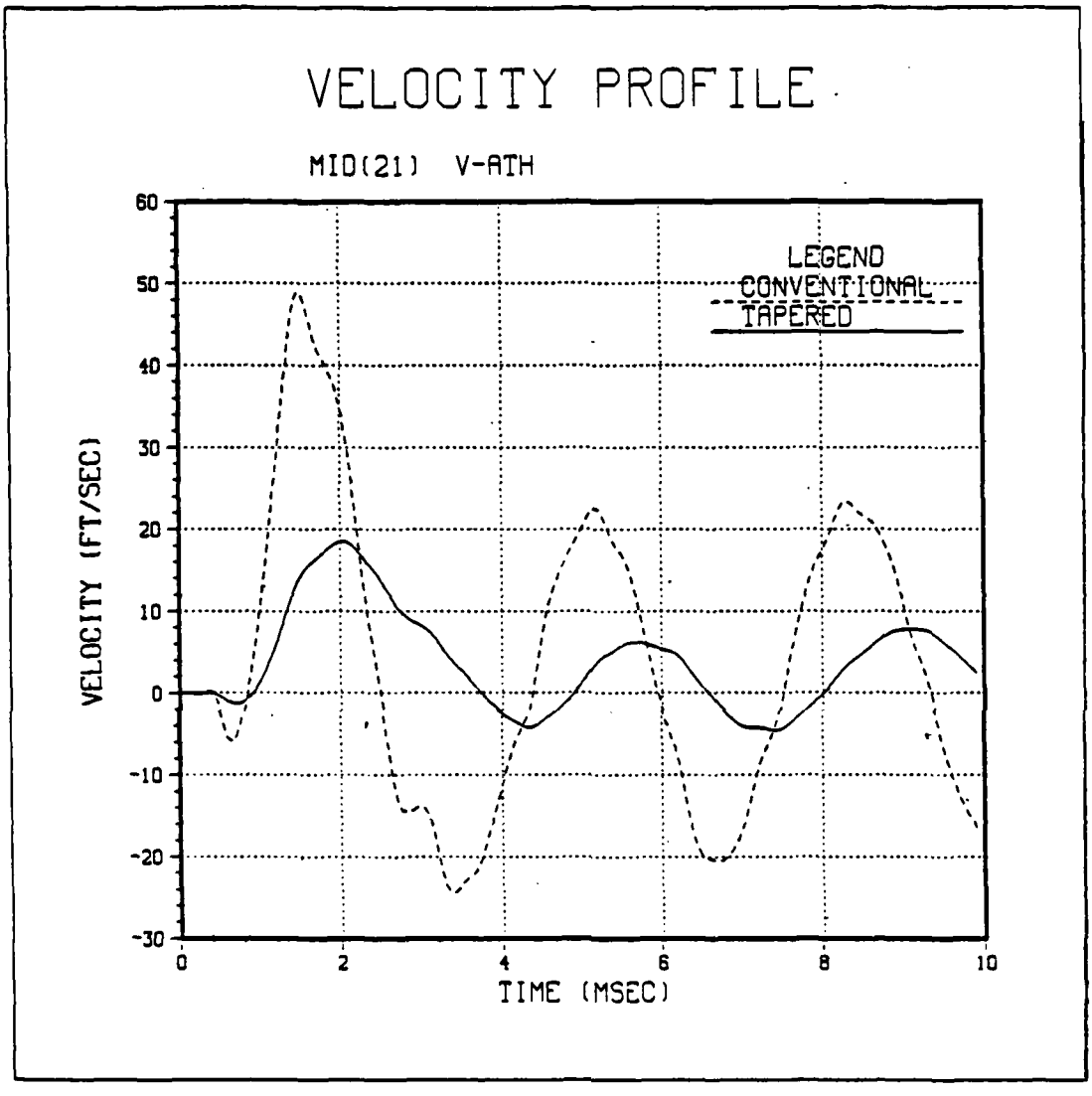

Figure 15. Velocity-Time Histories at Beam Midsection for D = 4.2 In.

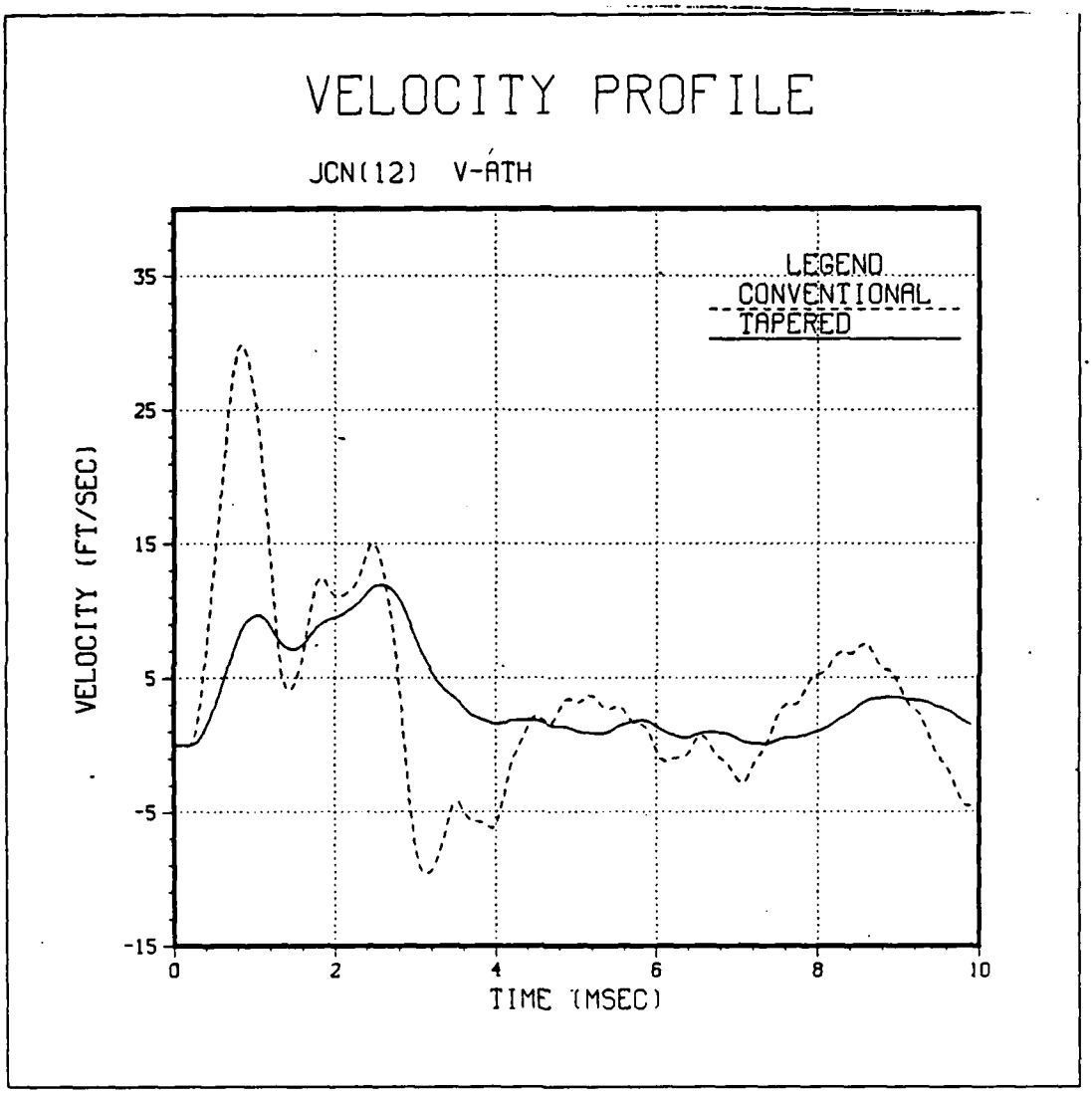

Figure 16. Velocity-Time Histories at Beam/Bracket Junction for D = 4.2 In.

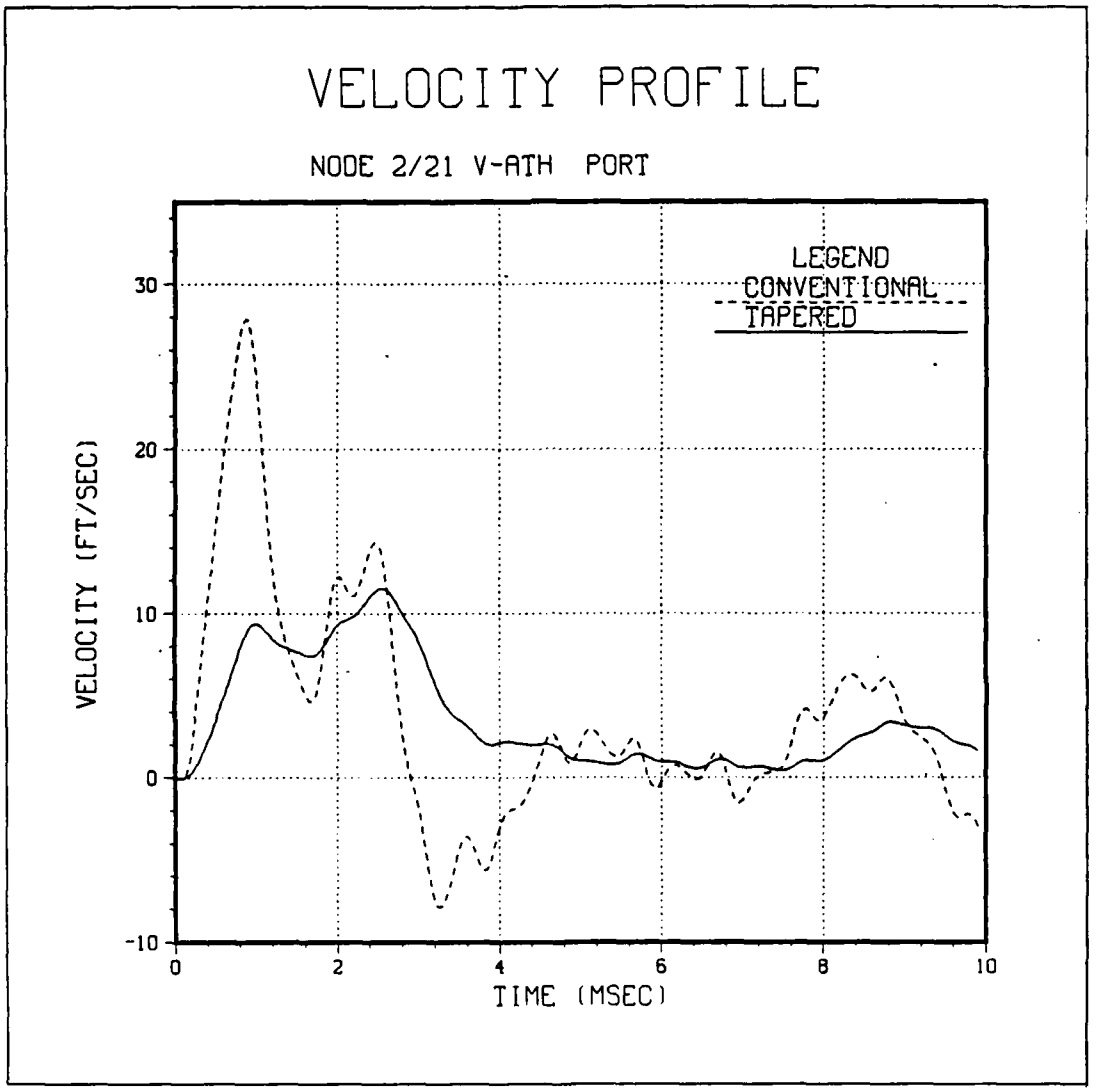

Figure 17. Velocity-Time Histories at Frame 18 for D = 4.2 In.

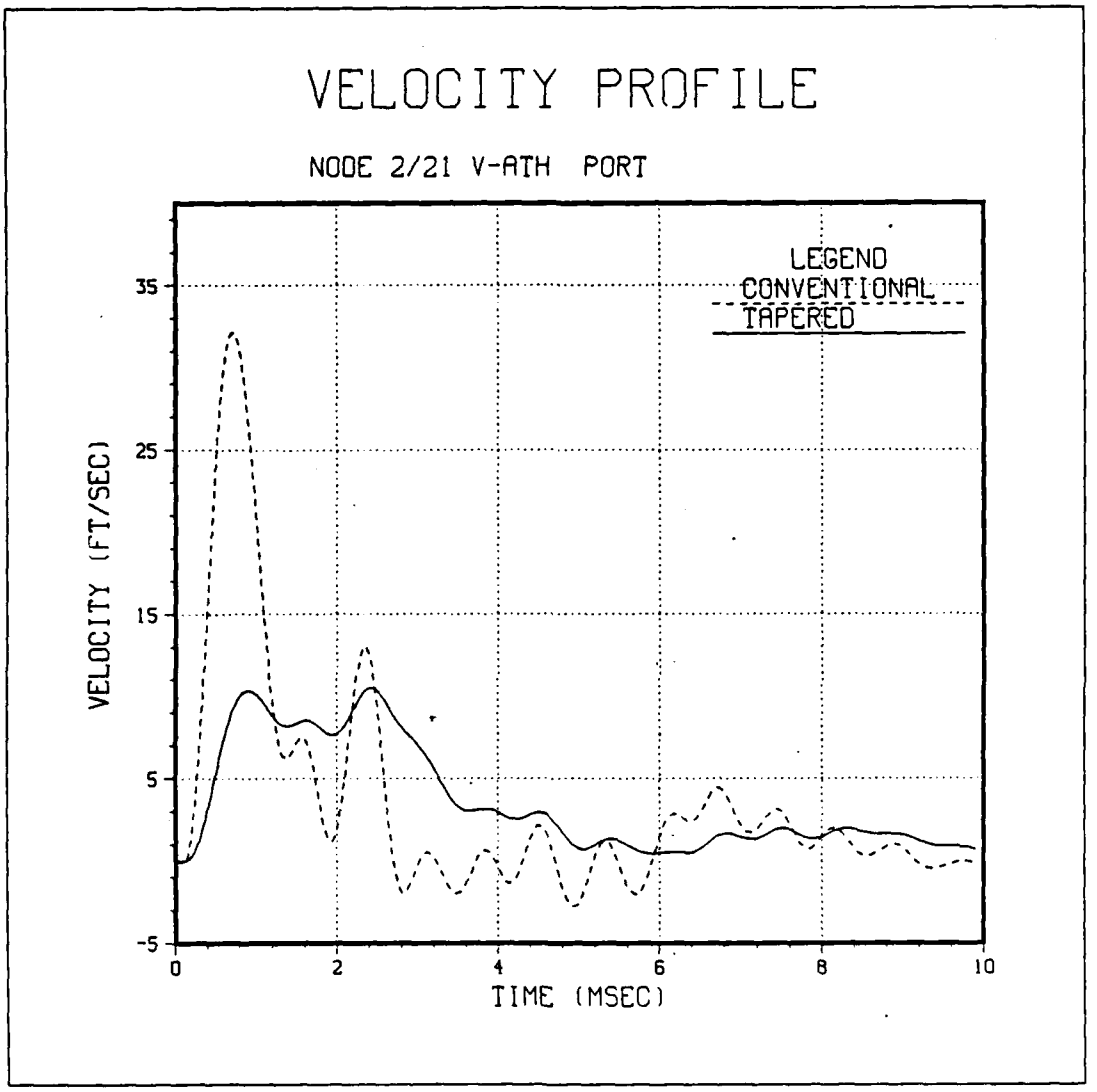

Figure 18. Velocity-Time Histories at Frame 18 for Empty Shell

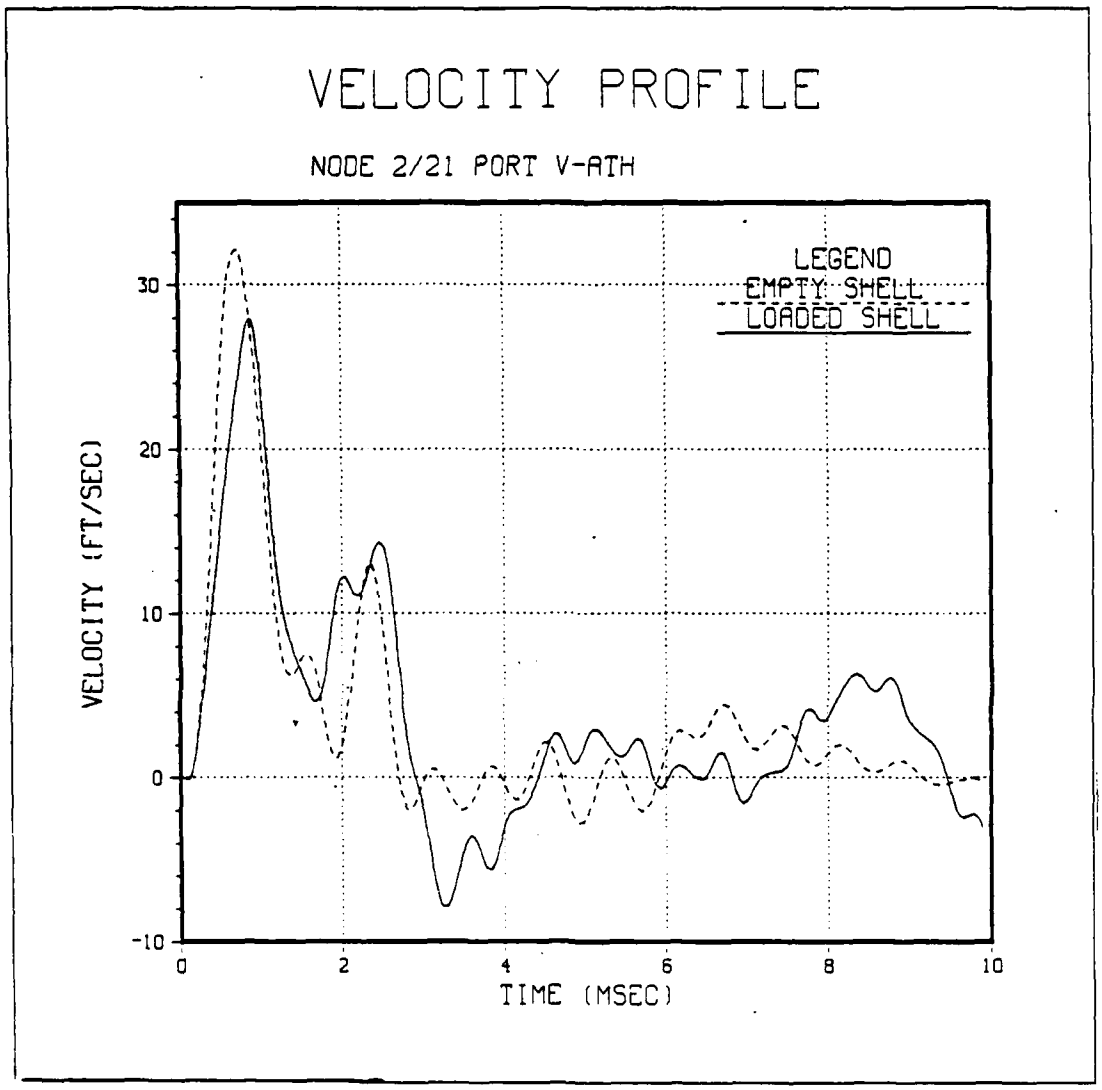

Figure 19. Velocity-Time Histories at Frame 18 for Conventional Charge

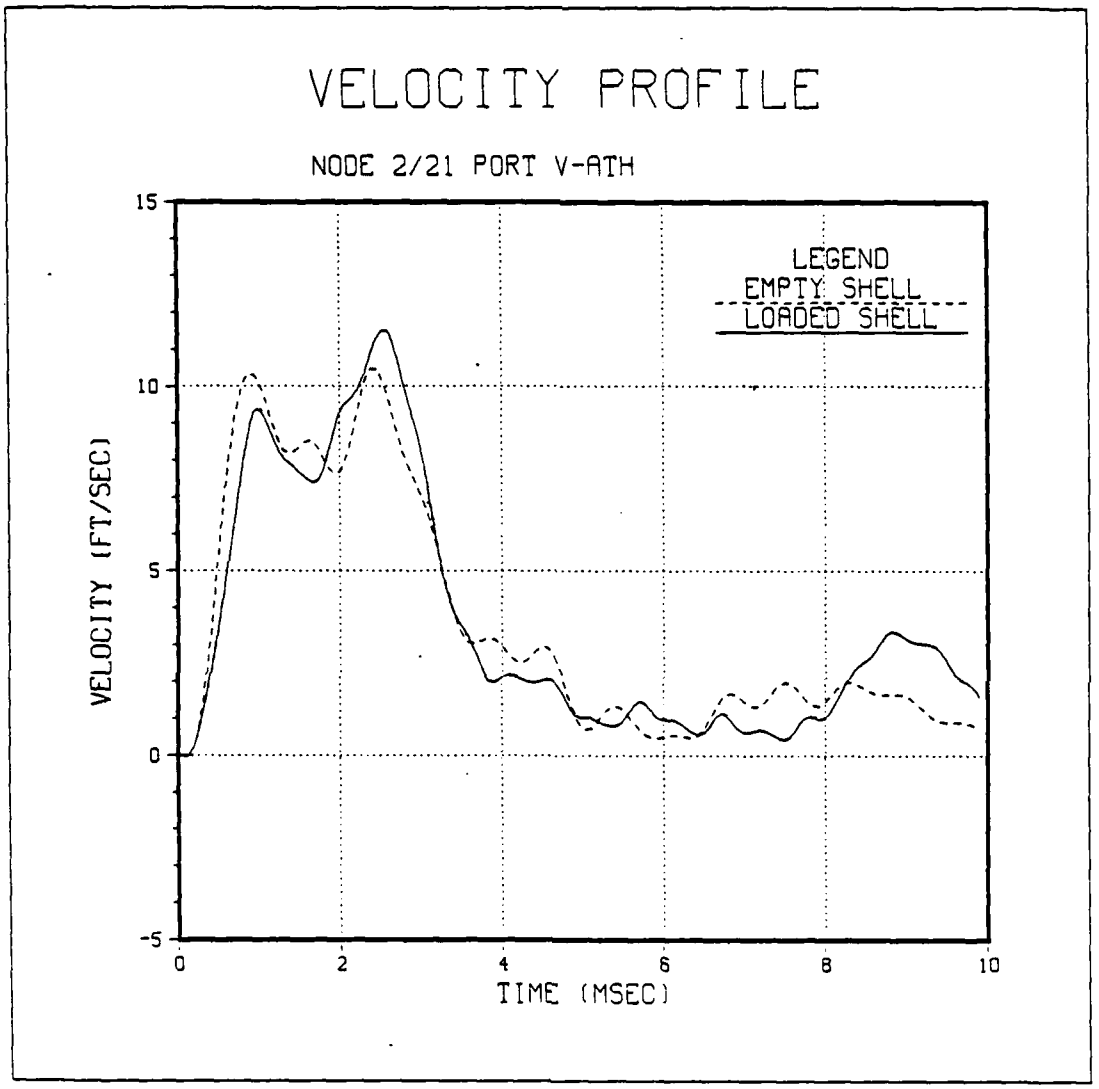

Figure 20. Velocity-Time Histories at Frame 18 for Tapered Charge

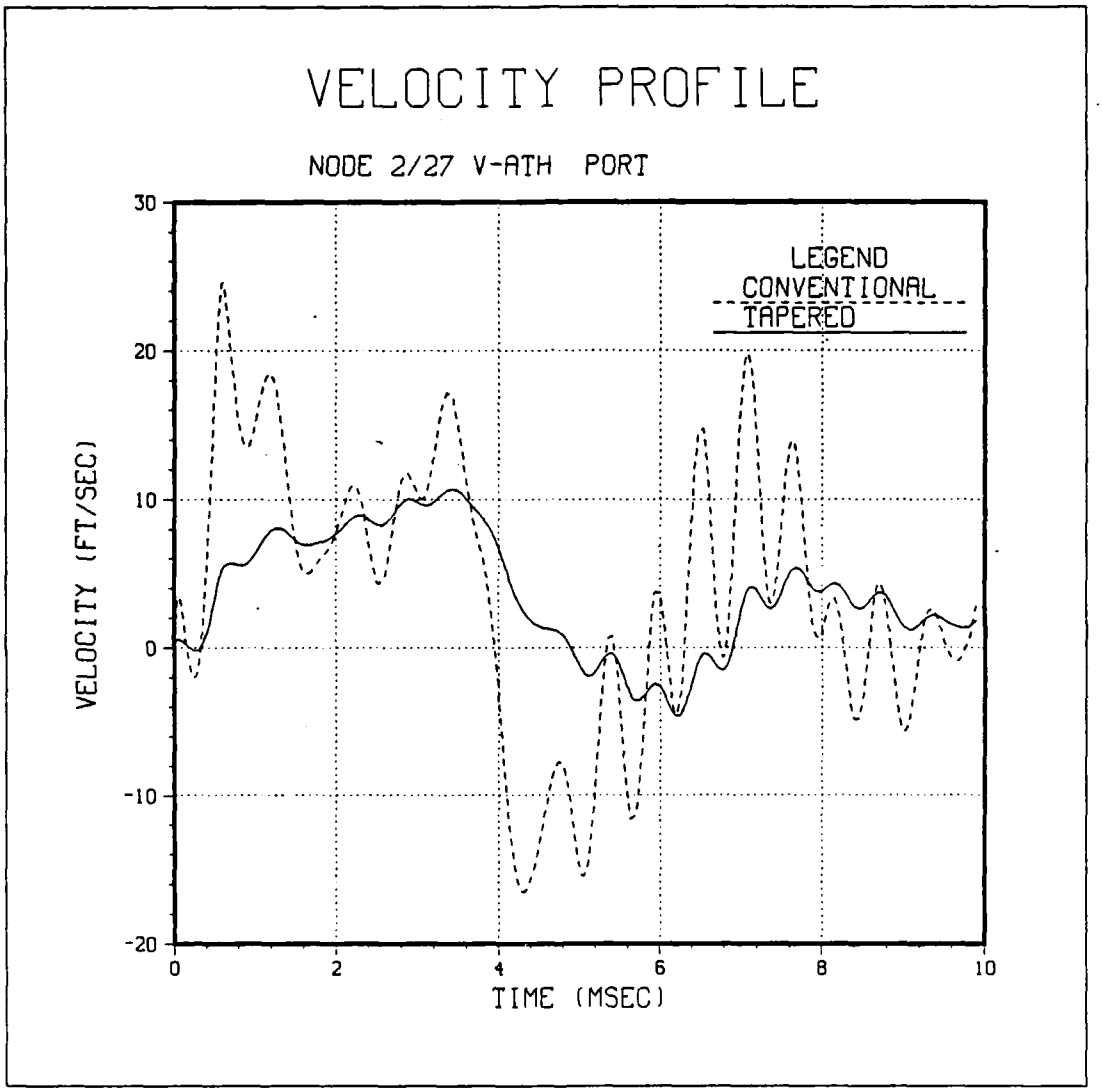

Figure 21. Velocity-Time Histories at Midships with Substructure of D = 4.2 In.

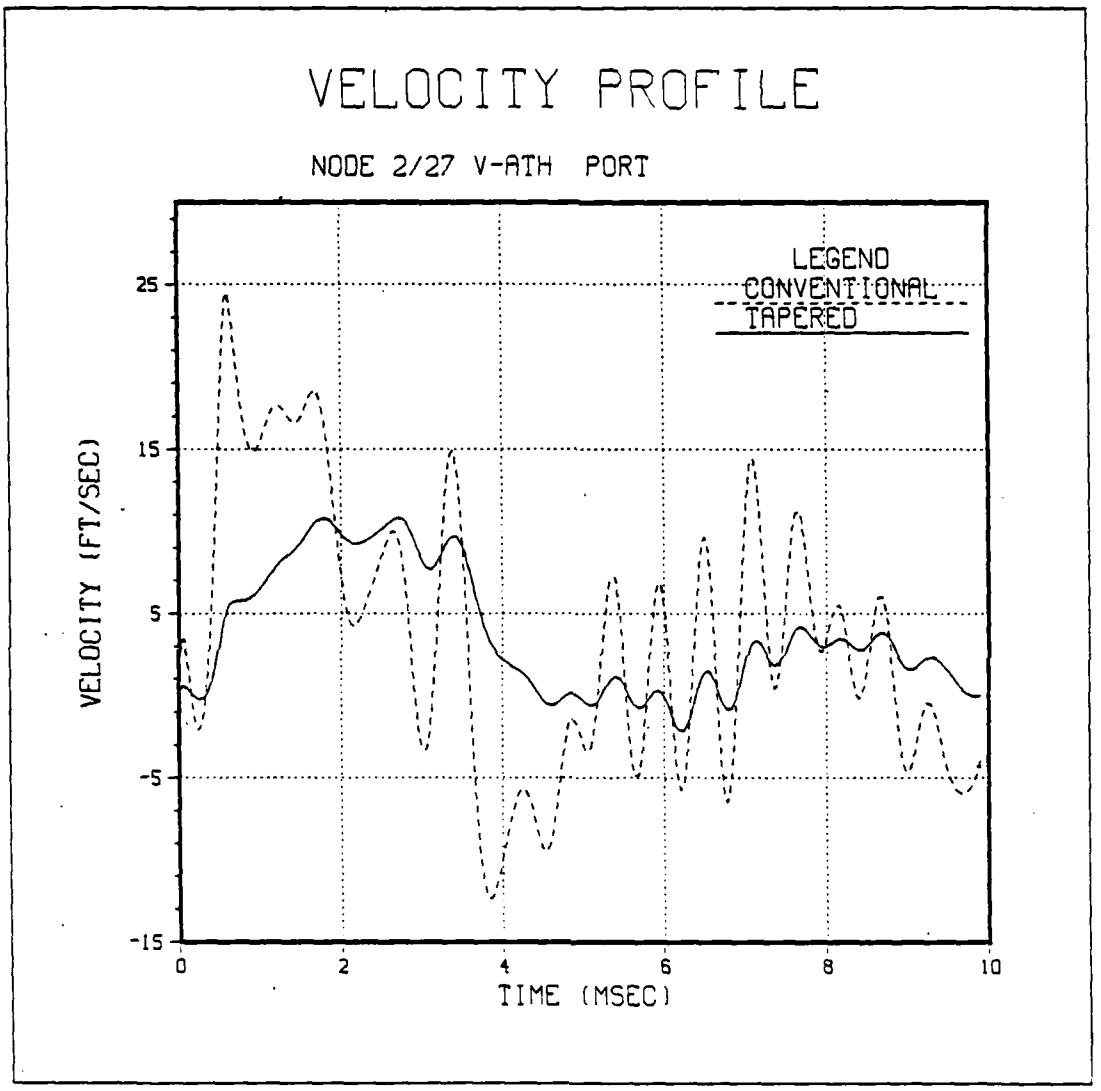

Figure 22. Velocity-Time Histories at Midships for Empty Shell

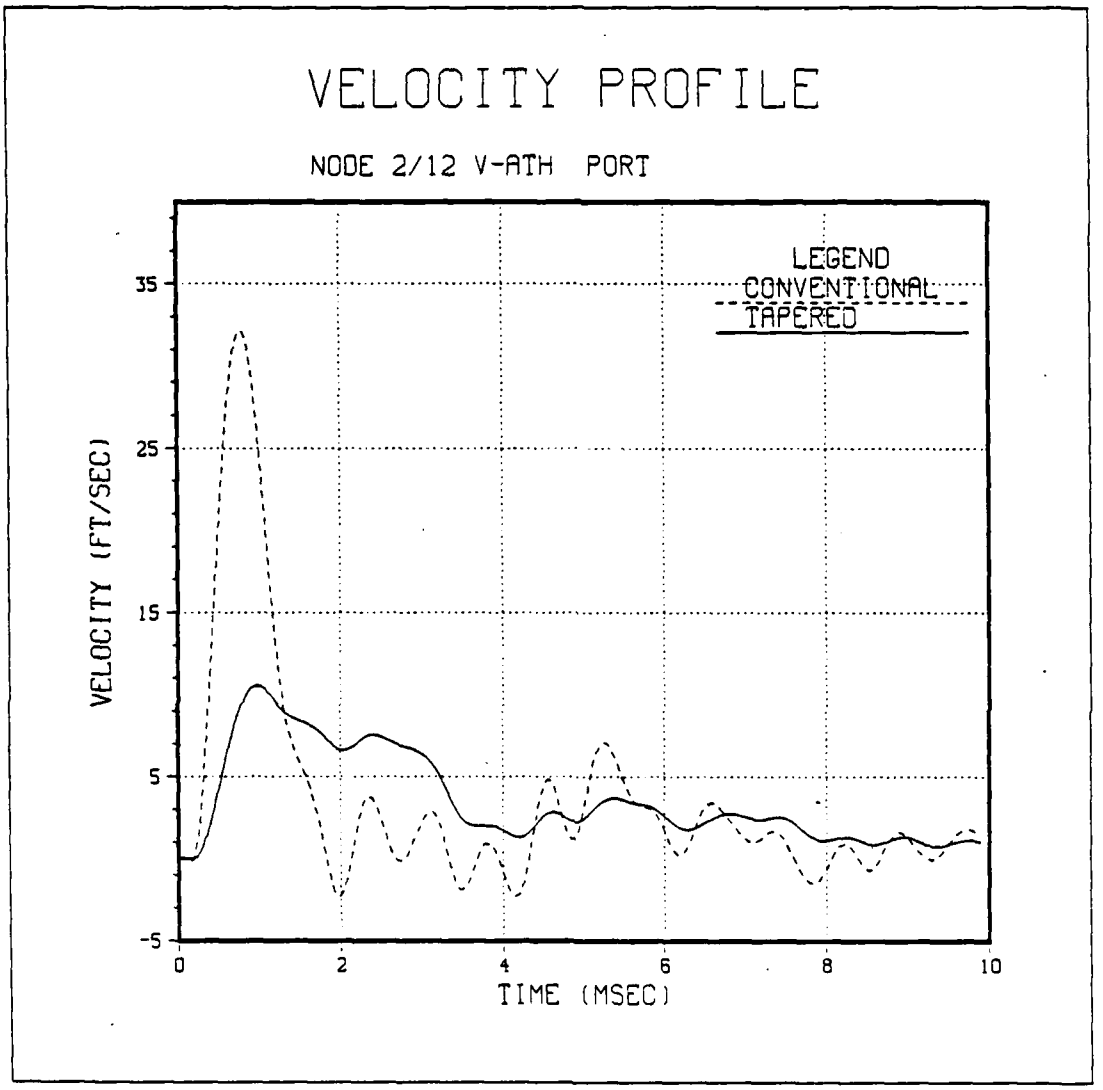

Figure 23. Velocity-Time Histories at Frame 9 for Empty Shell

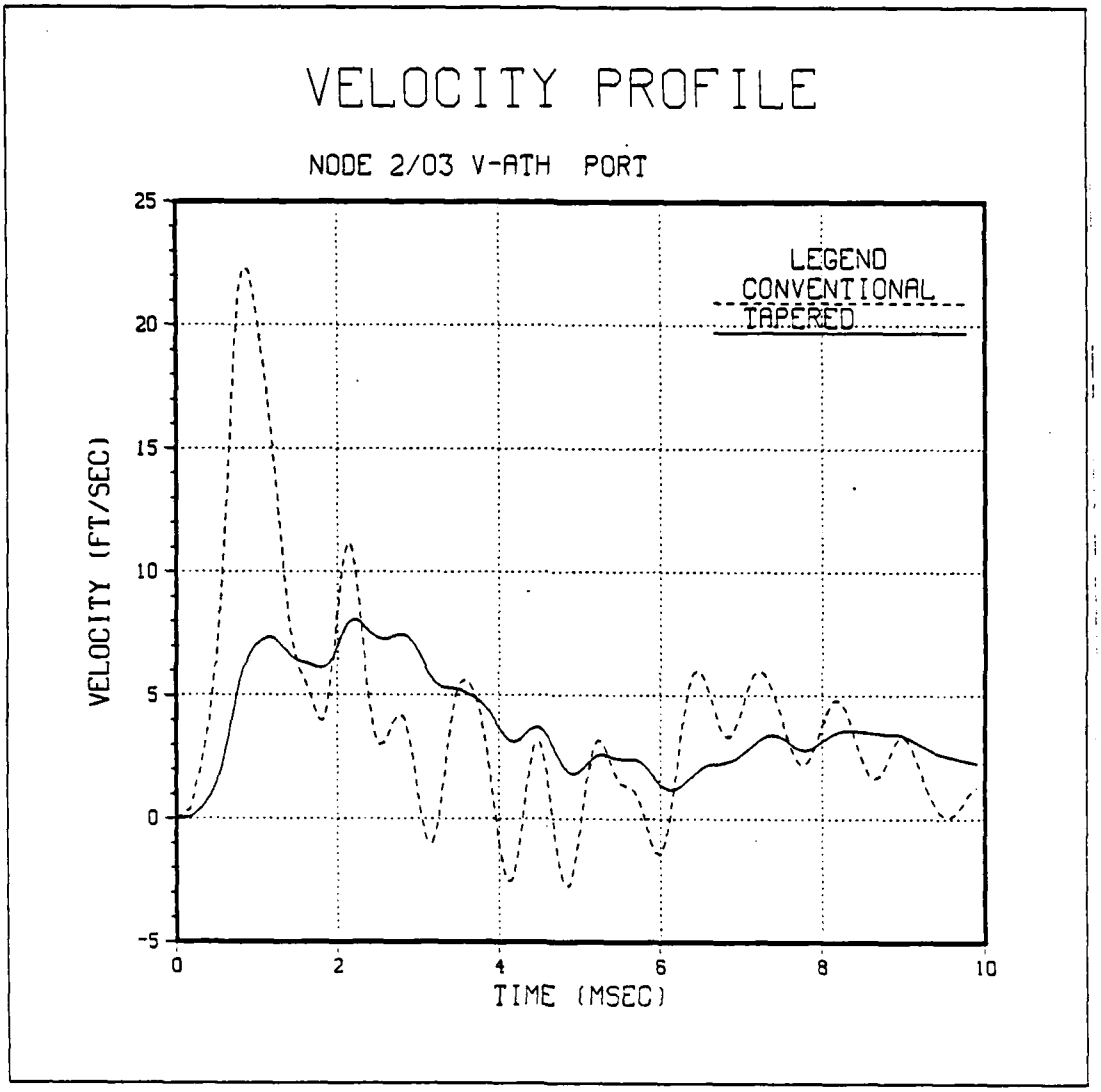

Figure 24. Velocity-Time Histories at Frame 0 for Empty Shell

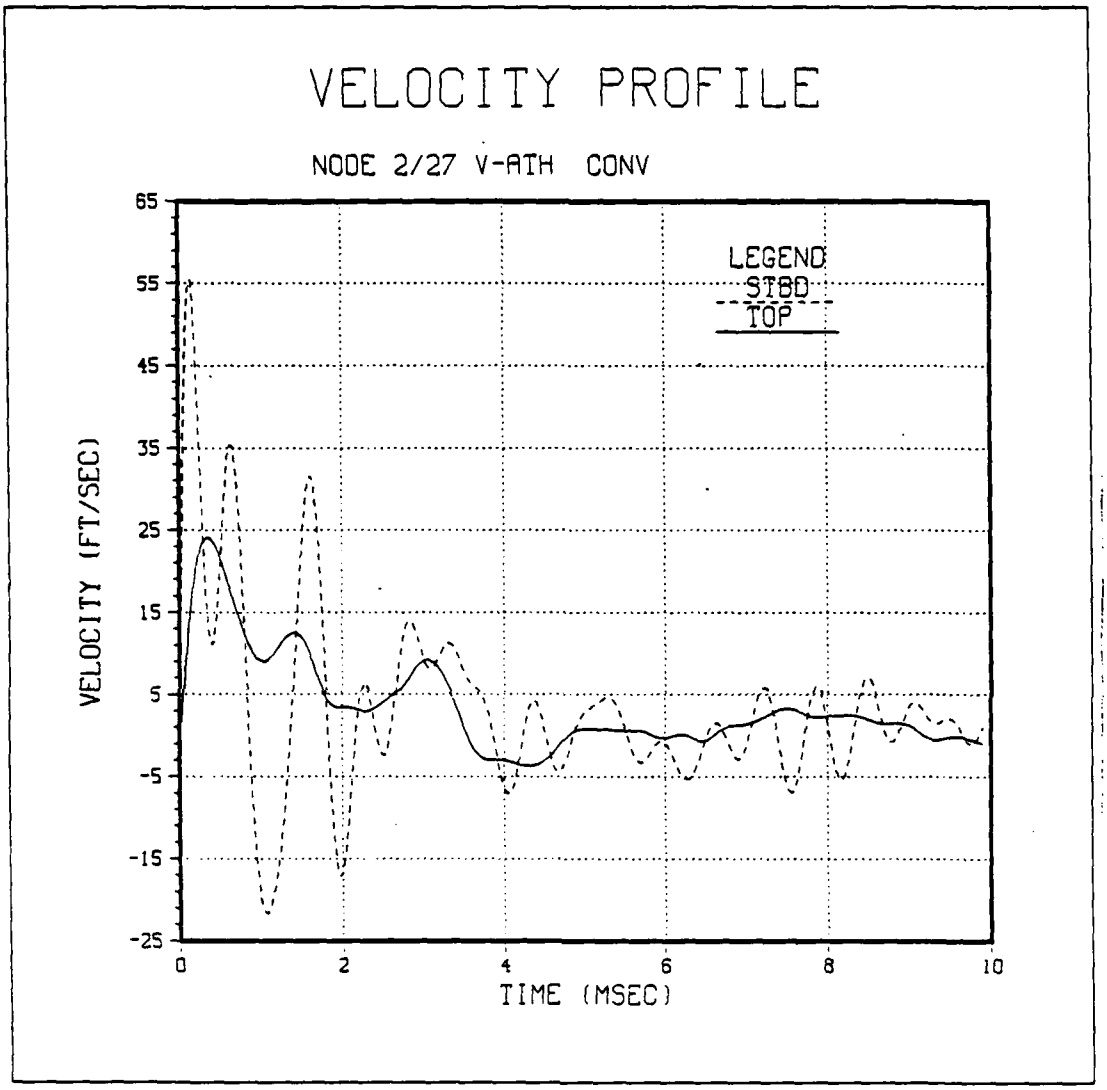

Figure 25. Velocity-Time Histories at Midships for Empty Shell from Conventional Charge

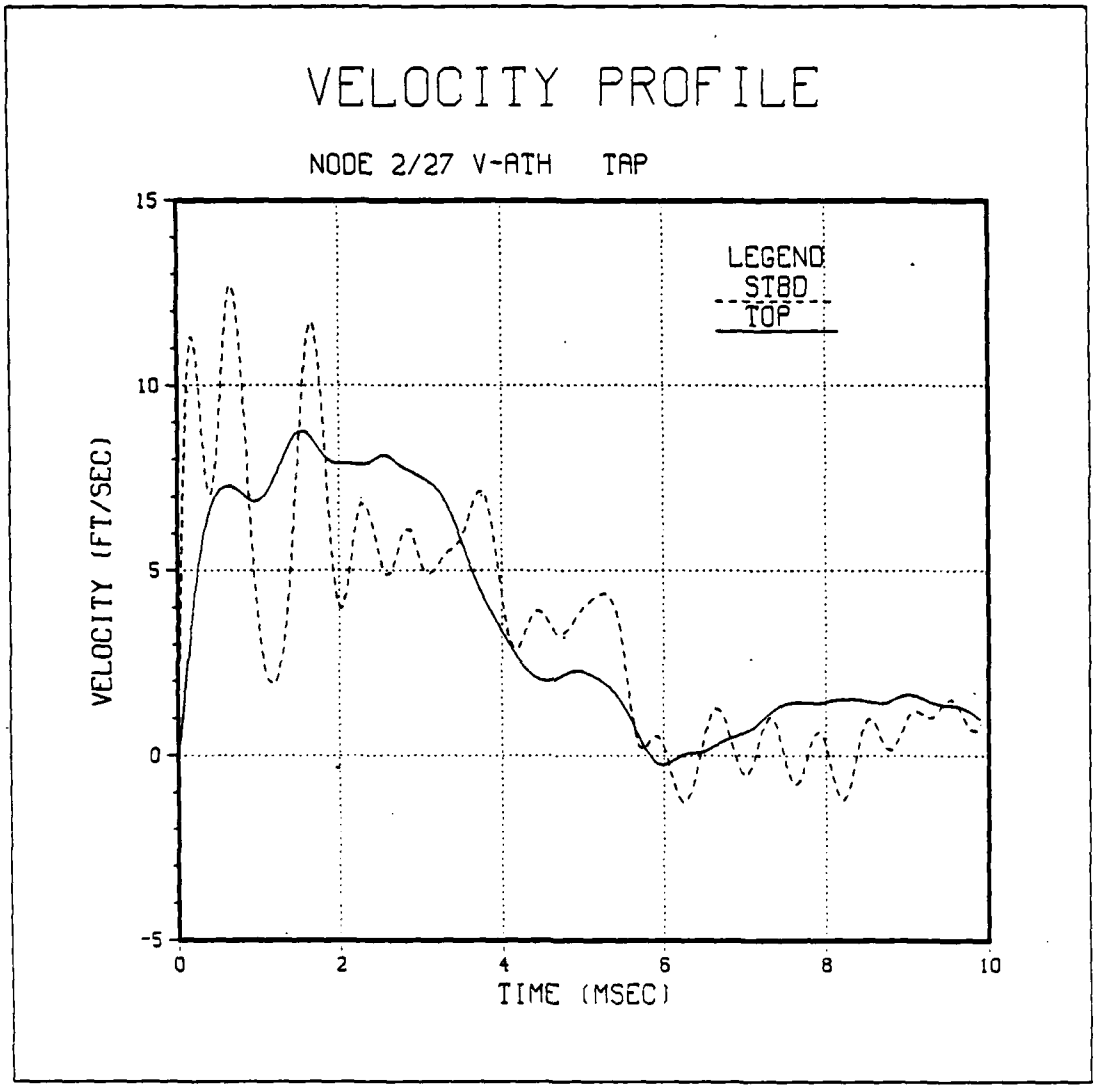

Figure 26. Velocity-Time Histories at Midships for Empty Shell from Tapered Charge

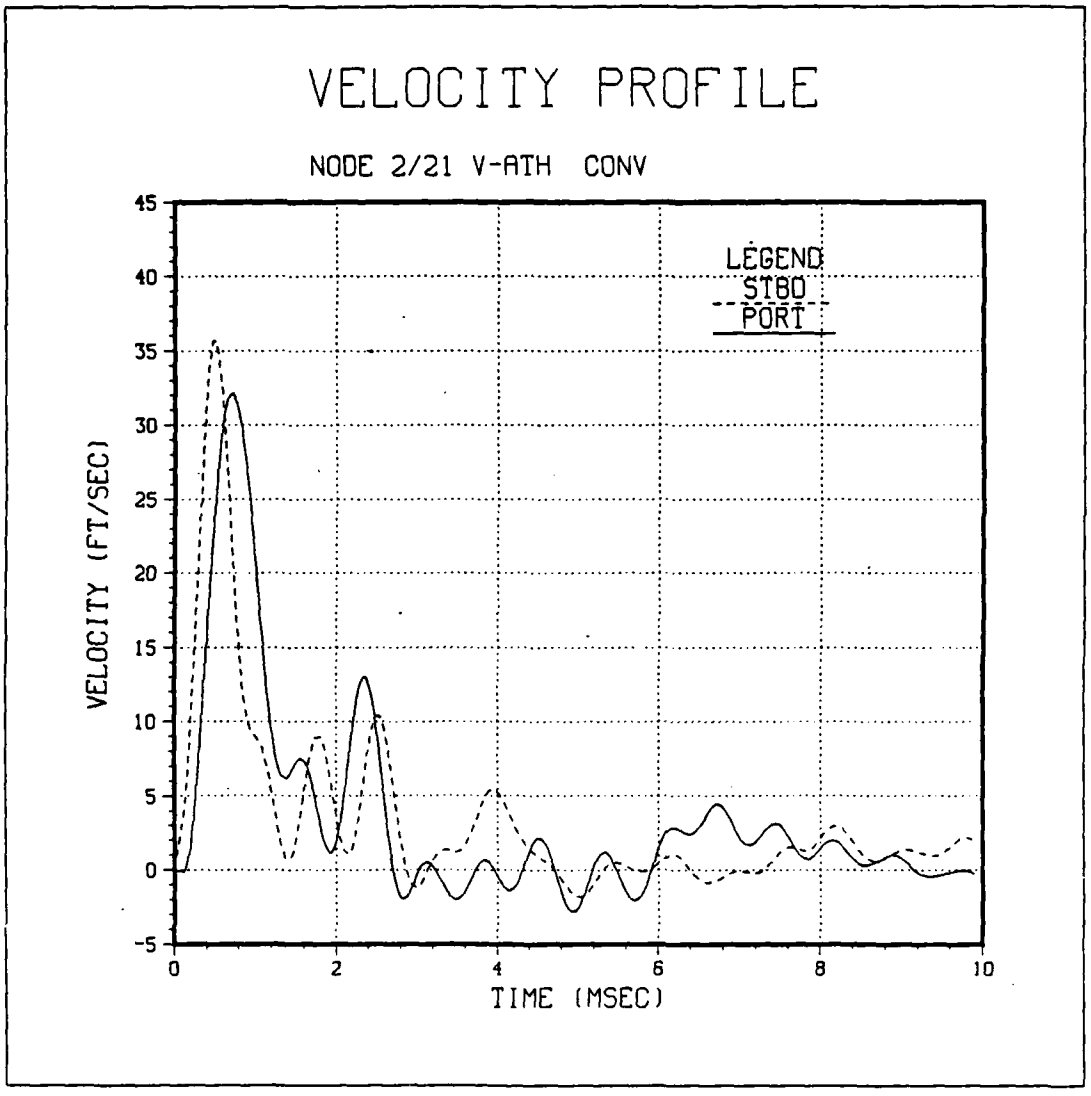

Figure 27. Velocity-Time Histories at Frame 18 of Empty Shell from Conventional Charge

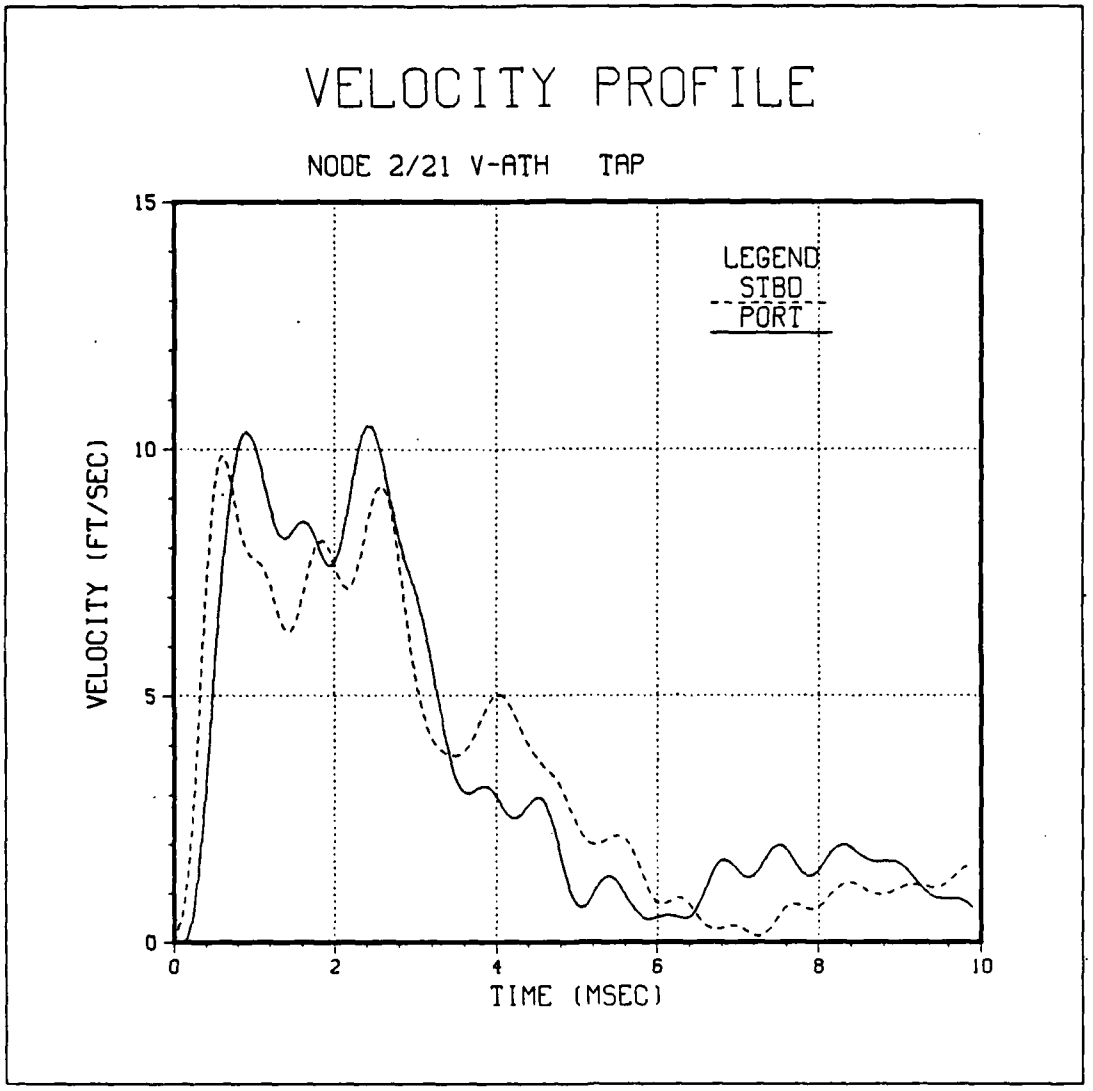

Figure 28. Velocity-Time Histories at Frame 18 of Empty Shell from Tapered Charge

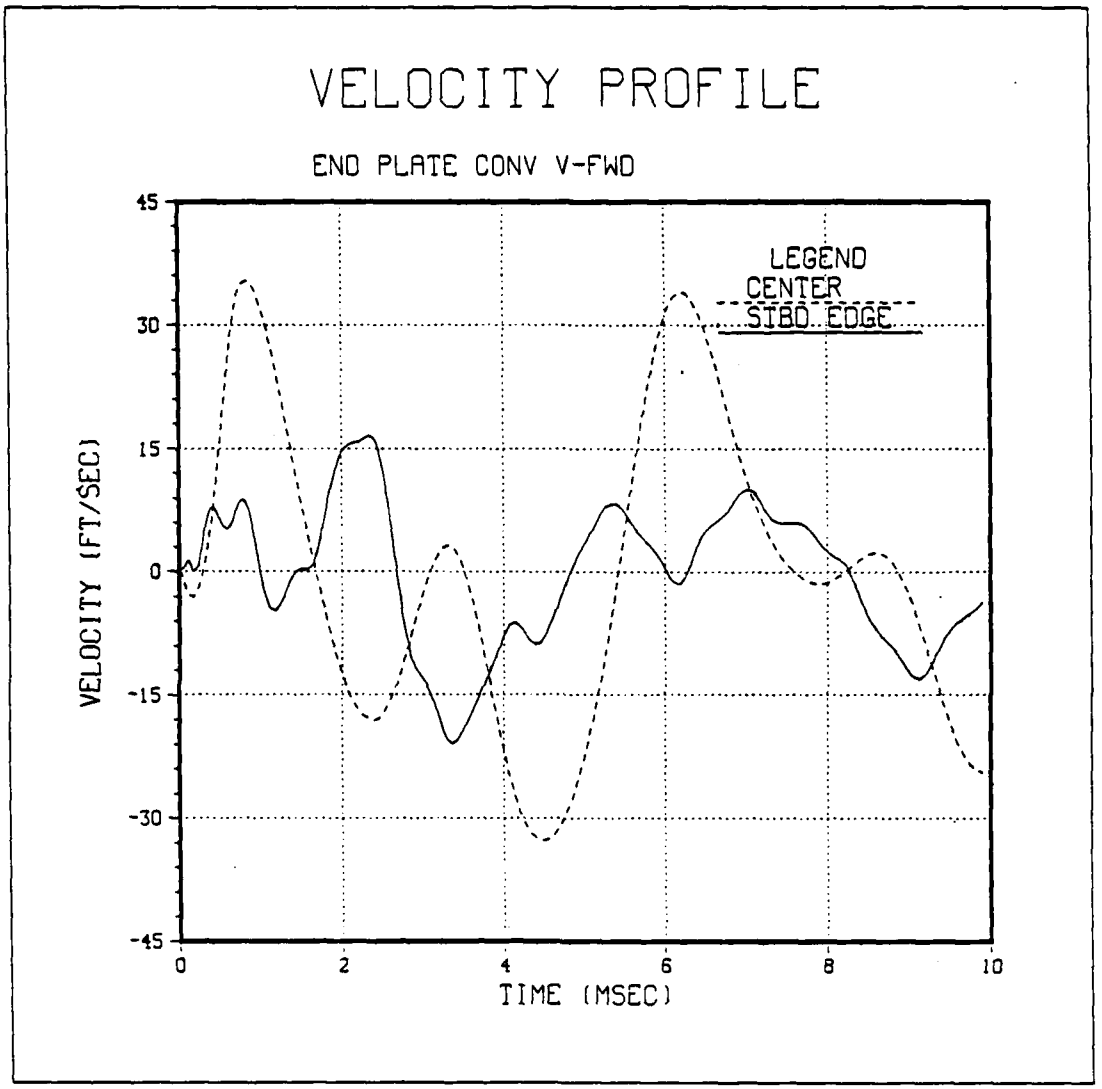

Figure 29. Velocity-Time Histories at End Plate for Conventional Charge

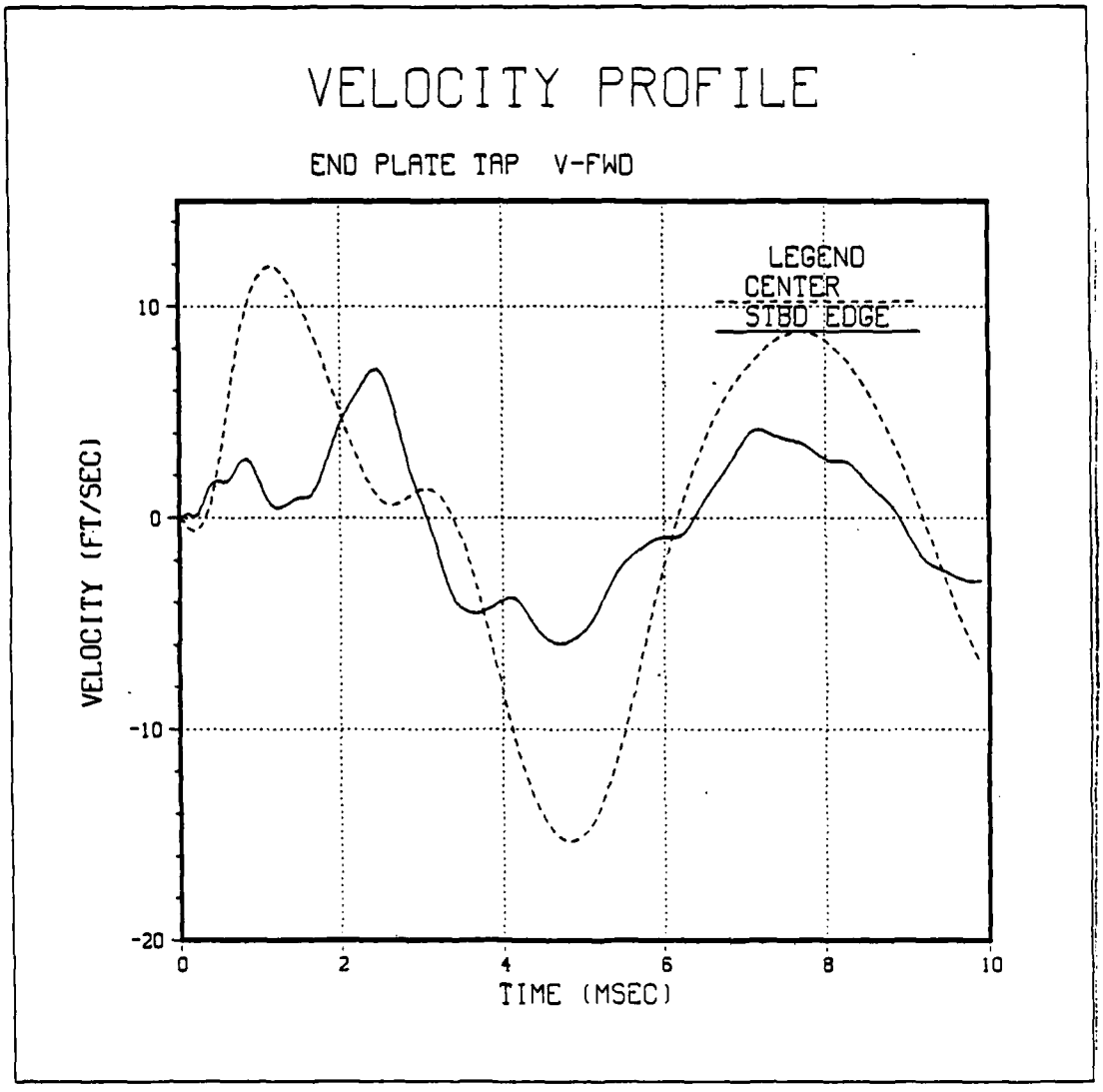

Figure 30. Velocity-Time Histories at End Plate for Tapered Charge

VI. CONCLUSIONS

The results from the cases studied tend to show that a model can be designed to minimize dynamic amplification. In no case did a truly resonant situation occur. As the substructure model increased in size and mass so did the stiffness and the effect was as if a lumped mass was attached to the shell. Even though substructure sizes having frequencies that matched those of the hull were tested, the corresponding mode shapes being excited did not result in dynamic amplification of the beam responses. The beam model having a secondary frequency of 330.5 Hz became slightly amplified but only for the conventional explosive analysis.

Though the models used in this study are based on real configurations it is important to keep in mind this was a numerical study on a simplified model of an already simple structure. Even though the substructure design used did not become highly excited when combined with the shell in this study, the beam's behavior might change if combined with a shell that has a frequency range and mode shapes that are different from those of the shell used in this study. The shell model was a relatively small structure that resulted in a majority of frequencies too high to excite the substructure significantly.

ELSHOK has the capability of representing much more complex models than those used here. It has the capability of simulating a full sized submarine hull with internally attached equipment. The ELSHOK code has been shown to give fairly accurate results, especially in the early portion of shock problems, through comparisons of its predictions to physical test results. However, like any numerical device it needs such comparisons to verify its results. On the other hand, conducting tests using ELSHOK has the distinct advantage of eliminating risk of damage to valuable assets. Once a model has been verified to satisfactorily predict the prototype responses, a variety of internal equipment models could be applied to perform a variety of studies at fractions of the cost of building real models. Again the drawbacks are the pitfalls of any numerical endeavor, namely, the output is only as good as the input. Simplified models may produce simplified results and poor assumptions must be guarded against.

It is important to realize that the results of this study were arrived at through the implementation of a potentially powerful tool for future research at the Naval Postgraduate School, namely ELSHOK. Further studies in the area of UNDEX using the code should be carried out to prove its validity or develop it into more useful applications of design and research. Suggestions on improvements to develop

the line of research in this thesis from a numerical sensitivity study into a realistic problem are to obtain or construct a representative full-size submarine model or SSTV for BOSOR4 and model all internal equipments to be tested in appropriate detail while applying fewer restrictions to the degrees of freedom.

LIST OF REFERENCES

1. Department of the Navy Military Specification MIL-S-901C (Navy), Shock Test, HI (High Impact) Shipboard Machinery, Equipment and Systems, Requirements for, 15 January 1983.

2. R. Vasudevan and D. Ranlet, Submerged Shock Responses of a Linearly Elastic Shell of Revolution Containing Internal Structures, User's Manual for the ELSHOK Code, Weidlinger Associates, New York, New York, May 1982.

3. Baron, M. L., Comments on the Design of the ONR Model, paper presented at the DNA/ONR/NAVSHIPS Shock Hardening Program, Alexandria, Virginia, 17 July 1974.

4. Cole, R. H., Underwater Explosions, pp. 210-242, Princeton University Press, 1948.

5. Ranlet, D., DiMaggio, F. L., Bleich, H. H., and Baron, M. L., "Elastic Responses of Submerged Shells with Internally Attached Structures to Shock Loading," International Journal of Computers and Structures, V. 7, No. 3, pp. 355-364, June 1977.

6. Geers, T. L., "Residual Potential and Approximate Methods for Three-Dimensional Fluid-Structure Interaction Problems," Journal of the Acoustical Society of America, V. 49, No. 5, (Part 2), pp. 1505-1510, 1971.

7. Bushnell, D., Stress, Stability and Vibration of Complex Branched Shells of Revolution: Analysis and User's Manual for BOSOR4, LMSC-D24 3605, Lockheed Missiles and Space Community, Inc., Sunnvale, California, March 1972.

8. Earthquake Engineering Research Center Report No. EERC 73-11, SAP IV-A Structural Analysis Program for Static and Dynamic Response of Linear Systems, by K. J. Bathe, E. L. Wilso and F. E. Peterson, University of California, Berkeley, California, April 1974.

9. Ranlet, D. DiMaggio, F.L., "Transient Response of Shells with Internally Attached Structures," International Journal of Computers and Structures, V. 9, No. 5, pp. 475-481, November 1978.

10. Nuclear Engineering Division General Electric Company NEDE-25494, Effects of Undesigned-For High-Frequency Vibrations on Plant Equipment Components, by Y. S. Shin, December 1981.

APPENDIX A

INPUT FILES FOR ELSHOK

1. BOSOR4 INPUT DATA FOR ALL CASES

The following data file was used to generate the cylindrical shell model. Four separate runs of BOSOR4 were made corresponding to N = 0,1,2,3 by setting NOB, NMINB and NMAXB equal to each case N. All other inputs remain the same for each case.

```
RING-STIFFENED CYLINDER WITH FLAT ENDPLATES--SYMMETRY USED--N=0
         2      $ INDIC = ANALYSIS TYPE INDICATOR
         1      $ NPRT = OUTPUT OPTIONS (1=MINIMUM, 2=MEDIUM, 3=MAXIMUM)
         0      $ ISTRES= OUTPUT CONTROL (0=RESULTANTS, 1=SIGMA, 2=EPSILON)
         2      $ NSEG  = NUMBER OF SHELL SEGMENTS (LESS THAN 25)
       H
       H        $ SEGMENT NUMBER     1     1     1     1     1     1     1     1
         7      $ NMESH = NUMBER OF NODE POINTS (5 = MIN., 98 = MAX.)( 1)
         3      $ NTYPEH= CONTROL INTEGER (1 OR 2 OR 3) FOR NODAL POINT SPACING
         1      $ NSHAPE= INDICATOR (1,2 OR 4) FOR GEOMETRY OF MERIDIAN
         0      $ R1    = RADIUS AT BEGINNING OF SEGMENT (SEE P. 66)
         0      $ Z1    = AXIAL COORDINATE AT BEGINNING OF SEGMENT
  16.81250      $ R2    = RADIUS AT END OF SEGMENT
         0      $ Z2    = AXIAL COORDINATE AT END OF SEGMENT
         0      $ IMP   = INDICATOR FOR IMPERFECTION (0=NONE, 1=SOME)
         3      $ NTYPEZ= CONTROL (1 OR 3) FOR REFERENCE SURFACE LOCATION
  2.500000      $ ZVAL  = DISTANCE FROM LEFTMOST SURF. TO REFERENCE SURF.
       N        $ DO YOU WANT TO PRINT OUT R(S), R'(S), ETC. FOR THIS SEGMENT?
         0      $ NRINGS= NUMBER (MAX=20) OF DISCRETE RINGS IN THIS SEGMENT
         0      $ K=ELASTIC FOUNDATION MODULUS (E.G. LB/IN**3)IN THIS SEG.
         0      $ LINTYP= INDICATOR (0, 1, 2 OR 3) FOR TYPE OF LINE LOADS
         0      $ NLTYPE=CONTROL (0,1,2,3) FOR TYPE OF SURFACE LOADING
         2      $ NWALL=INDEX (1, 2, 4, 5, 6, 7, 8) FOR WALL CONSTRUCTION
0.10800000E+08  $ E     = YOUNG'S MODULUS FOR SKIN
 0.3200000      $ U     = POISSON'S RATIO FOR SKIN
0.25350000E-03  $ SM =MASS DENSITY OF SKIN (E.G. ALUM.=.00025 LB-SEC**2/IN**4)
         0      $ ALPHA = COEFFICIENT OF THERMAL EXPANSION
         0      $ ANRS  = CONTROL (0 OR 1) FOR ADDITION OF SMEARED STIFFENERS
         1      $ SUR   = CONTROL FOR THICKNESS INPUT (0 OR 1 OR -1)
       N        $ DO YOU WANT TO PRINT OUT THE C(I,J) AT MERIDIONAL STATIONS?
       N        $ DO YOU WANT TO PRINT OUT DISTRIBUTED LOADS ALONG MERIDIAN?
       H
       H        $ SEGMENT NUMBER     2     2     2     2     2     2     2     2
        25      $ NMESH = NUMBER OF NODE POINTS (5 = MIN., 98 = MAX.)( 2)
         3      $ NTYPEH= CONTROL INTEGER (1 OR 2 OR 3) FOR NODAL POINT SPACING
         1      $ NSHAPE= INDICATOR (1,2 OR 4) FOR GEOMETRY OF MERIDIAN
  16.81250      $ R1    = RADIUS AT BEGINNING OF SEGMENT (SEE P. 66)
         0      $ Z1    = AXIAL COORDINATE AT BEGINNING OF SEGMENT
  16.81250      $ R2    = RADIUS AT END OF SEGMENT
  129.0625      $ Z2    = AXIAL COORDINATE AT END OF SEGMENT
         0      $ IMP   = INDICATOR FOR IMPERFECTION (0=NONE, 1=SOME)
         3      $ NTYPEZ= CONTROL (1 OR 3) FOR REFERENCE SURFACE LOCATION
 0.1875000      $ ZVAL  = DISTANCE FROM LEFTMOST SURF. TO REFERENCE SURF.
       N        $ DO YOU WANT TO PRINT OUT R(S), R'(S), ETC. FOR THIS SEGMENT?
         3      $ NRINGS= NUMBER (MAX=20) OF DISCRETE RINGS IN THIS SEGMENT
         2      $ NTYPE = CONTROL FOR IDENTIFICATION OF RING LOCATION (2=Z, 3=R)
  3.500000      $ Z(I)  = AXIAL COORDINATE OF ITH RING, Z( 1)
  53.12500      $ Z(I)  = AXIAL COORDINATE OF ITH RING, Z( 2)
  103.7500      $ Z(I)  = AXIAL COORDINATE OF ITH RING, Z( 3)
         1      $ NTYPER= TYPE (0 OR 1 OR 2 OR 4 OR 5) OF DISCRETE RING NO.( 1)
         1      $ NTYPER= TYPE (0 OR 1 OR 2 OR 4 OR 5) OF DISCRETE RING NO.( 2)
         1      $ NTYPER= TYPE (0 OR 1 OR 2 OR 4 OR 5) OF DISCRETE RING NO.( 3)
0.30000000E+08  $ E     = YOUNG'S MODULUS OF RING( 1)
  7.125000      $ A     = CROSS SECTION AREA OF RING( 1)
  7.535500      $ IY    = MOMENT OF INERTIA ABOUT Y-AXIS (SEE FIG. ON P.70)( 1)
  2.375000      $ IX    = MOMENT OF INERTIA ABOUT X-AXIS( 1)
         0      $ IXY   = PRODUCT OF INERTIA( 1)
 -1.781250      $ E1    = RADIAL COMPONENT OF RING ECCENTRICITY (SEE P. 70)( 1)
         0      $ E2    = AXIAL  COMPONENT OF RING ECCENTRICITY( 1)
  .7501E+08     $ GJ    = TORSIONAL RIGIDITY( 1)
0.73300000E-03  $ RM    = RING MATERIAL DENSITY (E.G. ALUMINUM=.0002535)( 1)
0.30000000E+08  $ E     = YOUNG'S MODULUS OF RING( 2)
  8.250000      $ A     = CROSS SECTION AREA OF RING( 2)
  11.69800      $ IY    = MOMENT OF INERTIA ABOUT Y-AXIS (SEE FIG. ON P.70)( 2)
  2.750000      $ IX    = MOMENT OF INERTIA ABOUT X-AXIS( 2)
         0      $ IXY   = PRODUCT OF INERTIA( 2)
 -2.062500      $ E1    = RADIAL COMPONENT OF RING ECCENTRICITY (SEE P. 70)( 2)
         0      $ E2    = AXIAL  COMPONENT OF RING ECCENTRICITY( 2)
0.92490000E+08  $ GJ    = TORSIONAL RIGIDITY( 2)
0.73300000E-03  $ RM    = RING MATERIAL DENSITY (E.G. ALUMINUM=.0002535)( 2)
0.30000000E+08  $ E     = YOUNG'S MODULUS OF RING( 3)
  8.250000      $ A     = CROSS SECTION AREA OF RING( 3)
```

```
 11.69800      $ IY     = MOMENT OF INERTIA ABOUT Y-AXIS (SEE FIG. ON P.70)( 3)
 2.750000      $ IX     = MOMENT OF INERTIA ABOUT X-AXIS( 3)
        0      $ IXY    = PRODUCT OF INERTIA( 3)
-2.062500      $ E1     = RADIAL COMPONENT OF RING ECCENTRICITY (SEE P. 70)( 3)
        0      $ E2     = AXIAL  COMPONENT OF RING ECCENTRICITY( 3)
0.92490000E+08 $ GJ     = TORSIONAL RIGIDITY( 3)
0.73300000E-03 $ RM     = RING MATERIAL DENSITY (E.G. ALUMINUM=.0002535)( 3)
        0      $ K=ELASTIC FOUNDATION MODULUS (E.G. LB/IN**3)IN THIS SEG.
        0      $ LINTYP= INDICATOR (0, 1, 2 OR 3) FOR TYPE OF LINE LOADS
        0      $ NLTYPE=CONTROL (0,1,2,3) FOR TYPE OF SURFACE LOADING
        2      $ NWALL=INDEX (1, 2, 4, 5, 6, 7, 8) FOR WALL CONSTRUCTION
0.30000000E+08 $ E      = YOUNG'S MODULUS FOR SKIN
0.30000000     $ U      = POISSON'S RATIO FOR SKIN
0.73300000E-03 $ SM =MASS DENSITY OF SKIN (E.G. ALUM.=.00025 LB-SEC**2/IN**4)
        0      $ ALPHA  = COEFFICIENT OF THERMAL EXPANSION
        1      $ ANRS   = CONTROL (0 OR 1) FOR ADDITION OF SMEARED STIFFENERS
        1      $ SUR    = CONTROL FOR THICKNESS INPUT (0 OR 1 OR -1)
     N         $ ARE THERE STRINGERS (PLEASE ANSWER Y OR N)?
     Y         $ ARE THERE RINGS (PLEASE ANSWER Y OR N)?
        0      $ K2   =CONTROL (0 OR 1) FOR INTERNAL OR EXTERNAL RINGS
0.30000000E+08 $ E2     = RING MODULUS
0.30000000     $ U2     = RING POISSON RATIO
0.73300000E-03 $ RGMD=  RING MASS DENSITY
     Y         $ IS THE RING CROSS SECTION CONSTANT IN THIS SEGMENT?
     Y         $ IS THE RING CROSS SECTION RECTANGULAR (Y OR N)?
 5.625000      $ D2     = ARC LENGTH BETWEEN ADJACENT RINGS (CONSTANT)
0.2500000      $ T2     = THICKNESS OF RING (CONSTANT)
 1.250000      $ H2     = HEIGHT OF RING (CONSTANT)
     N         $ DO YOU WANT TO PRINT OUT THE C(I,J) AT MERIDIONAL STATIONS?
     N         $ DO YOU WANT TO PRINT OUT DISTRIBUTED LOADS ALONG MERIDIAN?
     H         $
     H         $ GLOBAL DATA...
    -1         $ NLAST  = PLOT OPTIONS  (-1=NONE, 0=GEOMETRY, 1=U,V,W)
     0         $ NOB    = STARTING NUMBER OF CIRC. WAVES (BUCKLING ANALYSIS)
     0         $ NMINB  = MINIMUM NUMBER OF CIRC. WAVES  (BUCKLING ANALYSIS)
     0         $ NMAXB  = MAXIMUM NUMBER OF CIRC. WAVES  (BUCKLING ANALYSIS)
     1         $ INCRB  = INCREMENT IN NUMBER OF CIRC. WAVES (BUCKLING)
    30         $ NVEC   = NUMBER OF EIGENVALUES FOR EACH WAVE NUMBER
     0         $ P      = PRESSURE OR SURFACE TRACTION MULTIPLIER
     0         $ TEMP   = TEMPERATURE RISE MULTIPLIER
     0         $ OMEGA  = ANGULAR VEL. ABOUT AXIS OF REVOLUTION (RAD/SEC)
     1         $ NUMBER OF POLES (PLACES WHERE R=0) IN SEGMENT( 1)
     H         $
     H         $ CONSTRAINT CONDITIONS FOR SEGMENT NO.    1    1    1    1
     1         $ IPOLE = NODAL POINT NUMBER OF POLE, IPOLE( 1)
     0         $ AT HOW MANY STATIONS IS THIS SEGMENT CONSTRAINED TO GROUND?
     N         $ IS THIS SEGMENT JOINED TO ANY LOWER-NUMBERED SEGMENTS?
     0         $ NUMBER OF POLES (PLACES WHERE R=0) IN SEGMENT( 2)
     H         $
     H         $ CONSTRAINT CONDITIONS FOR SEGMENT NO.    2    2    2    2
     1         $ AT HOW MANY STATIONS IS THIS SEGMENT CONSTRAINED TO GROUND?
    25         $ INODE = NODAL POINT NUMBER OF CONSTRAINT TO GROUND, INODE( 1)
     1         $ IUSTAR=AXIAL DISPLACEMENT CONSTRAINT (0 OR 1 OR 2)
     0         $ IVSTAR=CIRCUMFERENTIAL DISPLACEMENT(0=FREE,1=0,2=IMPOSED)
     0         $ IWSTAR=RADIAL DISPLACEMENT(0=FREE,1=CONSTRAINED,2=IMPOSED)
     1         $ ICHI=MERIDIONAL ROTATION (0=FREE,1=CONSTRAINED,2=IMPOSED)
     0         $ D1     = RADIAL COMPONENT OF OFFSET OF GROUND SUPPORT
     0         $ D2     = AXIAL COMPONENT OF OFFSET OF GROUND SUPPORT
     Y         $ IS THIS CONSTRAINT THE SAME FOR BOTH PREBUCKLING AND BUCKLING?
     Y         $ IS THIS SEGMENT JOINED TO ANY LOWER-NUMBERED SEGMENTS?
     1         $ AT HOW MAY STATIONS IS THIS SEGMENT JOINED TO PREVIOUS SEGS.?
     1         $ INODE = NODE IN CURRENT SEGMENT (ISEG) OF JUNCTION, INODE( 1)
     1         $ JSEG   = SEGMENT NO. OF PREVIOUS SEGMENT INVOLVED IN JUNCTION
     7         $ JNODE = NODE IN PREVIOUS SEGMNT (JSEG) OF JUNCTION
     1         $ IUSTAR= AXIAL DISPLACEMENT (0=NOT SLAVED, 1=SLAVED)
     1         $ IVSTAR= CIRCUMFERENTIAL DISPLACEMENT (0=NOT SLAVED, 1=SLAVED)
     1         $ IWSTAR= RADIAL DISPLACEMENT (0=NOT SLAVED, 1=SLAVED)
     1         $ ICHI   = MERIDIONAL ROTATION (0=NOT SLAVED, 1=SLAVED)
     0         $ D1     = RADIAL COMPONENT OF JUNCTURE GAP
     0         $ D2     = AXIAL COMPONENT OF JUNCTURE GAP
     Y         $ IS THIS CONSTRAINT THE SAME FOR BOTH PREBUCKLING AND BUCKLING?
     Y         $ DO YOU WANT TO LIST OUTPUT FOR SEGMENT( 1)




     Y         $ DO YOU WANT TO LIST OUTPUT FOR SEGMENT( 2)
     N         $ DO YOU WANT TO LIST PREBUCKLING RESULTANTS AND RING FORCES?
     N         $ DO YOU WANT TO LIST FORCES IN THE DISCRETE RINGS, IF ANY?
```

2. ACESNID INPUT DATA FOR ALL CASES

The input data for ACESNID must encompass all waves N used for the BOSOR4 model. The waves are specified by NSTART-NFINISH.

```
VIRTUAL MASS FOR RING STIFFENED CYLINDER WITH FLAT ENDS, N=0,1,2,3
    0 3 1 1 0 /NSTART,NFINISH,NFREQ,NVMASS,NCHECK
    12 61 12 2 1 /NFLAT,NCYL,NRITE,NWBOSG,NSYMF
    2 3 12 0 0 /NORDER,NFENDS,NFCENT,NFCMPT,NOMIT
    9.59684E-5 5.833E4 0.005 /RHOFL,VSOUND,ERR
    1 1 1 1 1 1 0 1 1 1 /OUTPUT FLAGS
    1.0 /CPS(1)
    1 1 1 9 /SETS JSGBEG,JPTBEG,JSGEND,JPTEND LEFT
    2 1 2 27 /SETS JSGBEG,JPTBEG,JSGEND,JPTEND CENTRAL
    1 1 1 9 /SOURCES JSGBEG,JPTBEG,JSGEND,JPTEND LEFT
    2 1 2 27 /SOURCES JSGBEG,JPTBEG,JSGEND,JPTEND CYLINDER
```

3. PIFLASH INPUT DATA FOR ALL CASES

BOSSY100-103 are the shell mode files produced from the BOSOR4 runs. Note the deleted shell modes that were purely torsional for N = 0.

```
4 0 0 1 1 /NUMBER NTORSN NPTM NSYM NSYMP
2 2 2 2   /(NWETSEG(K),NUSESEG(K),K=1,2
386.4     /GRAVITY
BOSSY100  /SMF,N=0
BOSSY101  /SMF,N=1
BOSSY102  /SMF,N=2
BOSSY103  /SMF,N=3
22 30 30 30 / (NJUSE(J),J=1,NITEMS)
1 2 3 4 / (KORGS(K),K=1,NKORGS)
3 4 6 7 13 14 15 16 17 18 19 20 21 22 23 24 25 26 27 28 29 30
1 2 3 4 5 6 7 8 9 10 11 12 13 14 15 16 17 18 19 20 21 22 23 24 25
26 27 28 29 30
1 2 3 4 5 6 7 8 9 10 11 12 13 14 15 16 17 18 19 20 21 22 23 24 25
26 27 28 29 30
1 2 3 4 5 6 7 8 9 10 11 12 13 14 15 16 17 18 19 20 21 22 23 24 25
26 27 28 29 30 / (JUSE(J,K), J=NJUSE(K))
```

4. SAP IV INPUT DATA FOR D = 4.2 IN. CASE

The following data file generated the internal structure model. Note that only half the doubly overhung beam is modeled as indicated by the beam lengths at the node, i.e., node 21 -- 44.81250.

```
SYMMETRICAL SUBSTRUCTURE--FOR BEAM OF D=4.2 IN
 21 1 0 10 1 0 0 0 0 0 /NUMP,NELTYP...NRIGID
 0 1 1 1 0 1 1 1 20.0 0.0 16.71875 0 0.0 /GEOMETRY AND DOF
 0 3 1 1 0 1 1 1 20.0 0.0 5.5729167 1 0.0
 0 4 1 1 0 1 0 1 0.0 0.0 0.0 0 0.0
 0 12 1 1 0 1 0 1 20.0 0.0 0.0 0 0.0
 0 13 1 1 0 1 0 1 22.756944 0.0 0.0 0 0.0
 0 20 1 1 0 1 0 1 42.055556 0.0 0.0 1 0.0
 0 21 1 1 0 1 1 1 44.81250 0.0 0.0 0 0.0
 2 20 2 0 2 7 2 BEAMS 20 ELEMTENTS TOTAL
 1 29.0E+06 0.3 7.29E-04 0.0/BEAM MOD,PQIS,DENS,,
 2 29.0E+06 0.3 7.29E-04 0.0 /BRACKET
 1 8.4 0.0 0.0 0.0 1.0 2.8 12.35/BEAM AREA AND MOMENTS OF I
 2 6.3 0.0 0.0 0.0 1.0 20.84 .525/BRACKET
 0.0 0.0 0.0 0.0 0.0 0.0
 0.0 0.0 0.0 0.0 0.0 0.0
 0.0 0.0 0.0 0.0 0.0 0.0 / MUULT G-X,Y,Z
 1 1 2 21 2 2 0 0 0 0 0 0 0 0
 2 2 3 21 2 2 0 0 0 0 0 0 0 0
 3 3 12 21 2 2 0 0 0 0 0 000000 000001 0/SET NODE RELEASE AT 12
 4 4 5 1 1 1 0 0 0 0 0 0 0 0
 20 20 21 1 1 1 0 0 0 0 0 0 0 0
 0 0 0.0 0.0 0.0 0.0 0.0 0.0 0.0 0.0 /CONC MASSES
 0.0 0.0 0.0 0.0 0.0 0.0 /ELEMENT LOAD MULTIPLIERS
 0 0 0 0.0 0.0 0.0 0.0 0.0 /IFPR,IFSS,...,NFO,SHIFT
 1 1 /NFACE,NSYM
 1 1 1 1 1 1 1 /NODE,(FIXITY(J),J=1,6
END DATA FOR D (DUMMY TITLES)
 0 0 0 0 0 0 0 0 0 0 0
```

5. PICRUST INPUT DATA FOR D = 4.2 IN. CASE

The circumferential location of the substructure attachment point is specified by ANDEG which is the angle ccw from the shell global Z-axis. The meridional location is specified by the node 21 at frame 18. The angle DEGROT specifies the orientation of the substructure local z-axis to the shell Z-axis. This is indicated by α_σ in Figure 5.

```
1 1 1 1 0 1 1 1 0 0
0 1 1 1 1 1 0 1 0 1 /OUTPUT FLAGS 1-20
5 0 0 /NJUSE,NHWSOB,NHWBAR
1 2 21 180.0 /NIPSUB,LBOSEG,LBOSPT,ANDEG
180.0 / DEGROT
1 2 3 4 5 / (JUSE(J),J=1,NJUSE)
```

6. USLOB INPUT DATA

In Phase III of ELSHOK the USLOB code performs the integration of the incident pressures using a Runge-Kutta scheme. NCHARGE specifies which type of UNDEX is to be represented. For the tapered charge nine discrete pressure-time points are used as input. The numbers following the charge weight of 352 lb. are the constants used in equations (1) and (2) that empirically describe the explosive HBX-1 (order-K1, K2, K3, K4). Note the 0.0 for surface cutoff effects. For the empty shells NSUBS must be set to 0. The integration is performed to compute velocities at all the nodes that make up the shell and substructure but only a couple are requested as printed output in NPTSH and NPTSUB as indicators that the program ran successfully. Nodes 1/01 and 2/21 are checked on the shell and node 1 and 21 are checked on the substructure. The value NQUAN = 3 requests the z direction velocities as output.

```
TAPERED CHARGE
  331 2 2 9 5 1 1 /NTIME,NSKIP,NCHARGE,NQUAD,NFINE,KOUPLE,NSUBS
  3.0E-05 129.0625 856.8125 0.0 /DELT,XLOAD,RLOAD,SURCUT
  9 /NSHAPE
  0.0 240.0 .0002 320.0 .00053 350.0 .00243 305.0 .00294 160.0
 .00340 115.0 .0044 70.0 .00540 48.0 .00565 0.0/DISCRETE POINT INPUTS
  0.0 /DECAY
  1 0 1 0 0 1 0 1 0 1
  1 0 1 0 1 0 1 0 1 0 /OUTPUT FLAGS 1-20
  2 /NPTSHL
  1 1 2 21 /LBOSEG,LBOSPT
  2 /NPTSUB
  1 3 21 3 /NSTAT,NQUAN
```

```
CONVENTIONAL CHARGE
 331 2 1 9 5 1 1/NTIME,NSKIP,NCHRG,...,NSUBS
 3.0E-05 129.0625 856.8125 0.0/DELT,XLOAD,RLOAD,SURCUT
 352 3.835E+05 1.144 3.031E-05 -0.247
 1 0 1 0 1 0 1 0 1 1
 1 1 1 0 0 0 1 0 1 1/OUTPUT FLAGS
 2/NPTSHL
 1 1 2 21/LBOSEG,LBSPOT
 2/NPTSUB/NSTAT,NQUAN
 1 3 21 3
```

7. PUSLOB INPUT DATA

This data file generates the velocity profiles that are plotted on Tektronix devices. The time step DELT and the interval of integration specified by NTIME and NSKIP must be the same as for USLOB. This input requests velocity profiles be expressed in terms of the shell global coordinate system. Shell output is requested by segment node and angle. Each substructure point is specified by node, number of degrees of freedom at the node for which velocity profiles are to be produced and which degree of freedom it is produced for. The tip is node 4, one degree of freedom in the local z direction.

```
331 2 1 1 1/NTIM,NSKIP,NSUBS,NTEK,NCARD
3.0E-05 1000.0 1.0/DELT,XMULT,YMULT
VELOCITY PROFILE D=4.2/TITLE OF PLOT
TIME (MSEC)
VELOCITY *IN/SEC*
16/NPTSHL-W
V-ATH 1/01
1 1 -1 1 0.0
V-ATH 1/04
1 4 -1 2 0.0 180.0
V-ATH 1/09
1 9 1 2 0.0 180.0
V-ATH 2/03
2 3 1 2 0.0 180.0
V-ATH 2/07
2 7 1 2 0.0 180.0
V-ATH 2/12
2 12 1 2 0.0 180.0
V-ATH 2/16
2 16 1 2 0.0 180.0
V-ATH 2/21
2 21 1 2 0.0 180.0
V-ATH 2/27
2 27 1 2 0.0 180.0
V-ATH 1/09
1 9 1 2 90.0 270.0
V-ATH 2/03
2 3 1 1 90.0
V-ATH 2/07
2 7 1 1 90.0
V-ATH 2/12
2 12 1 1 90.0
V-ATH 2/16
2 16 1 1 90.0
V-ATH 2/21
2 21 1 1 90.0
V-ATH 2/27 /SUB TITLE OF PLOT
2 27 1 1 90.0 /LBOSEG,LBOSPT,NSPHC,NANG,ANGDEG
16/NPTSHL-U
V-FWD 1/01
1 1 1 1 0.0
V-FWD 1/04
1 4 1 2 0.0 180.0
V-FWD 1/09
1 9 1 2 0.0 180.0
```

```
V-FWD 2/03
2 3 -1 2 0.0 180.0
V-FWD 2/07
2 7 -1 2 0.0 180.0
V-FWD 2/12
2 12 -1 2 0.0 180.0
V-FWD 2/16
2 16 -1 2 0.0 180.0
V-FWD 2/21
2 21 -1 2 0.0 180.0
V-FWD 2/27
2 27 -1 2 0.0 180.0
V-FWD 1/09
1 9 1 2 90.0 270.0
V-FWD 2/03
2 3 -1 1 90.0
V-FWD 2/07
2 7 -1 1 90.0
V-FWD 2/12
2 12 -1 1 90.0
V-FWD 2/16
2 16 -1 1 90.0
V-FWD 2/21
2 21 -1 1 90.0
V-FWD 2/27
2 27 -1 1 90.0
16/NPTSHL-V


V-DWN 1/01
1 1 -1 1 0.0
V-DWN 1/04
1 4 -1 2 0.0 180.0
V-DWN 1/09
1 9 -1 2 0.0 180.0
V-DWN 2/03
2 3 -1 2 0.0 180.0
V-DWN 2/07
2 7 -1 2 0.0 180.0
V-DWN 2/12
2 12 -1 2 0.0 180.0
V-DWN 2/16
2 16 -1 2 0.0 180.0
V-DWN 2/21
2 21 -1 2 0.0 180.0
V-DWN 2/27
2 27 -1 2 0.0 180.0
V-DWN 1/09
1 9 -1 2 90.0 270.0
V-DWN 2/03
2 3 -1 1 90.0
V-DWN 2/07
2 7 -1 1 90.0
V-DWN 2/12
2 12 -1 1 90.0
V-DWN 2/16
2 16 -1 1 90.0
V-DWN 2/21
2 21 -1 1 90.0
V-DWN 2/27
2 27 -1 1 90.0
3/NPTSUB
TIP (04)/NGAGE
 4 1 3/NSTAT,NDOFPT,NQUAN
JCN (12)
 12 1 3
MID (21)
 21 1 3
```

APPENDIX B

PROGRAMS USED TO PREPARE AND PLOT VELOCITY PROFILES

```
      PROGRAM PLOTCONV
C
CCCCC THE PURPOSE OF THIS PROGRAM IS TO READ THE PUNCH-CARD
CCCCC FILE FROM PUSLOB AND CONVERT IT TO A FORMAT WHICH CAN
CCCCC BE ACCEPTED BY EASYPLOT OR DISSPLA ON IBM 3033.
C
      DIMENSION VEL(166,32), VELO(166,2), LABEL(32), TAG(32), LTITLE(32)
      CHARACTER*10 LABEL
      CHARACTER*40 LTITLE
      COMMON/CSOLVE/DTRECS
      NCURV=32
      DO 10 K=1,NCURV
      READ(11,999) LTITLE(K),NRECS,DTRECS
      READ(11,998) LABEL(K), TAG(K)
      READ(11,997) (VEL(J,K), J=1,NRECS)
   10 CONTINUE
  999 FORMAT(A40,I5,1PE11.4)
  998 FORMAT(A10,F10.5)
  997 FORMAT(1P7E11.4)
      DO 20 L=1,NCURV
      T=0.0
      LL=L+20
      DO 30 M=1,NRECS
      VELO(M,1)=T
      DTRECS1=1000.0*DTRECS
      T=T+DTRECS1
      VELO(M,2)=VEL(M,L)/12.0
   30 CONTINUE
      DO 40 KK=1,NRECS
      WRITE(LL,996) (VELO(KK,JJ),JJ=1,2)
   40 CONTINUE
      WRITE(LL,995) LTITLE(L),NRECS,DTRECS
      WRITE(LL,994) LABEL(L),TAG(L)
   20 CONTINUE
  996 FORMAT(2F15.5)
  995 FORMAT(A40,I5,1PE11.4)
  994 FORMAT(A10,F10.5)
      STOP
      END
```

```
C     PROGRAM FISH1 IS THE FORTRAN CODE REQUIRED TO PLOT
      VELOCITY PROFILES USING DISSPLA
      REAL*4 VEL(166),TIM(166),TIM2(166),VEL2(166)
      DO 10 I=1,166
      READ(20,*)TIM(I),VEL(I)
   10 CONTINUE
      DO 20 J=1,166
      READ(21,*)TIM2(J),VEL2(J)
   20 CONTINUE
      CALL COMPRS
      CALL PAGE(8.0,8.0)
      CALL AREA2D(6.,5.5)
      CALL XNAME('TIME (MSEC)$',100)
      CALL YNAME('VELOCITY (FT/SEC)$',100)
      CALL HEADIN('VELOCITY PROFILE $',100,2.,1)
      CALL FRAME
      CALL INTAXS
      CALL YAXANG(0.)
      CALL YTICKS(5)
      CALL XTICKS(5)
      CALL GRAF(0.,2.0,10.,-10.,10.,35.)
      CALL MESSAG('NODE 2/21 PORT V-ATH  C$',23,1.,5.7)
      CALL LINESP (1.75)
      CALL LINES ('EMPTY SHELLS$',IPAK,1)
      CALL LINES ('LOADED SHELLS$',IPAK,2)
      XW=XLEGND (IPAK,2)
      YW=YLEGND (IPAK,2)
C     CALL MYLGEN ('KEY   $',100)
      CALL LEGLIN
      CALL POLY3
      CALL DASH
      CALL CURVE(TIM,VEL,166,0)
      CALL RESET('DASH')
      CALL CURVE(TIM2,VEL2,166,0)
      CALL DOT
      CALL GRID(1,1)
      CALL RESET('DOT')
      CALL LEGEND (IPAK,2,4.0,4.5)
      CALL ENDPL(0)
      CALL DONEPL
      STOP
      END
```

AD-A167 893 A PARAMETRIC STUDY OF ELASTIC RESPONSE OF SUBMARINE-INSTALLED EQUIPMENT S..(U) NAVAL POSTGRADUATE SCHOOL MONTEREY CA G F DECONTO MAR 86 2/2

UNCLASSIFIED F/G 13/10.1 NL

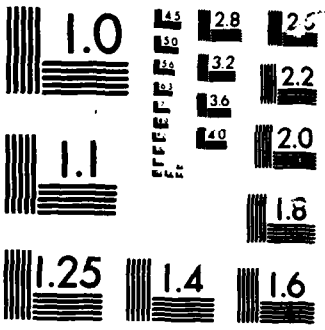

MICROCOPY CHART

APPENDIX C

PROGRAM USED TO ESTIMATE AXIAL FORCES IN THE SUPPORT BRACKETS

```
C       PROGRAM FORCES
C       ESTIMATES FORCES DEVELOPED IN THE SUPPORT BRACKETS
C       USING SIMPS 1/3  INTGRTR TO EST DEFLECTIONS
      REAL*4 TT(166),TB(166),VT(166,2),VB(166,2),X(166,2),XDEF(166)
      REAL*4 XL,EMOD,H,AREA,VT0,VT1,VT2,VB0,VB1,VB2,DT,DB,DEF
      REAL*4 XFORC,TIME,D
      XL=10.4
      EMOD=.3E+08
      D=4.2
      AREA=D*1.5
      H=6.0E-05
      DO 10 I=1,166
      READ(81,*) (VT(I,M),M=1,2)
      READ(82,*) (VB(I,N),N=1,2)
   10 CONTINUE
      DO 20 J=1,165,2
      II=J
      JJ=II+1
      KK=II+2
      VT0=VT(II,2)
      VT1=VT(JJ,2)
      VT2=VT(KK,2)
      VB0=VB(II,2)
      VB1=VB(JJ,2)
      VB2=VB(KK,2)
      DT=(VT0+4.*VT1+VT2)*H*4.0
      DB=(VB0+4.*VB1+VB2)*H*4.0
      DEF=(DT-DB)
      XFORC=(DEF/XL)*EMOD*AREA
      X(J,2)=XFORC
      TIME=VT(JJ,1)
      X(J,1)=TIME
      XDEF(J)=DEF
   20 CONTINUE
      DO 25 LL=1,163,2
      WRITE(6,*) (X(LL,MM),MM=1,2)
      WRITE(6,*) XDEF(LL)
   25 CONTINUE
      WRITE(83,*)   ' MSEC                LBF
      DO 30 L=1,163,2
      WRITE(83,*) (X(L,NN),NN=1,2)
   30 CONTINUE
      STOP
      END
```

TAPERED CHARGE

MSEC	LBF
5.9999999E-02	245.0312
0.1800000	-4871.925
0.3000000	-19920.20
0.4200000	-22457.08
0.5400000	-16749.71
0.6600000	-5310.641
0.7800000	5320.271
0.9000000	4192.220
1.020000	7970.726
1.140000	13106.43
1.260000	62.28399
1.380000	-14969.11
1.500000	-13569.19
1.620000	3981.250
1.740000	25546.64
1.860000	24680.42
1.980000	8301.491
2.100000	5590.140
2.220000	9395.421
2.340000	9359.116

CONVENTIONAL CHARGE

MSEC	LBF
5.9999999E-02	1461.115
0.1800000	-30141.24
0.3000000	-102820.2
0.4200000	-81457.16
0.5400000	-31330.44
0.6600000	35335.74
0.7800000	74938.54
0.9000000	40918.55
1.020000	54392.00
1.140000	65419.58
1.260000	-25939.18
1.380000	-89322.17
1.500000	-47749.70
1.620000	62073.85
1.740000	155272.9
1.860000	95783.45
1.980000	-15545.27
2.100000	-12975.48
2.220000	14247.56
2.340000	13262.66

2.460000	10169.69	2.460000	18125.72
2.580000	11816.05	2.580000	22709.01
2.700000	18961.72	2.700000	30505.12
2.820000	19368.80	2.820000	21335.82
2.940000	-382.3864	2.940000	-103091.1
3.060000	-13737.00	3.060000	-140059.4
3.180000	-8604.939	3.180000	-64635.81
3.300000	-2495.676	3.300000	-7922.625
3.420000	446.2275	3.420000	14542.41
3.540000	-3972.923	3.540000	-10436.12
3.660000	-9858.912	3.660000	-35627.13
3.780000	-5315.625	3.780000	-6730.258
3.900000	-6726.142	3.900000	-28879.58
4.020000	-15112.29	4.020000	-71626.63
4.140000	-11547.92	4.140000	-23481.91
4.260000	-4874.153	4.260000	31006.96
4.380000	-3058.313	4.380000	42378.32
4.500000	-4332.930	4.500000	24937.62
4.620000	-11046.69	4.620000	-21828.76
4.740000	-8562.529	4.740000	-1085.286
4.860000	2656.177	4.860000	59473.24
4.980000	1821.597	4.980000	39020.46
5.100000	-2468.413	5.100000	13899.35
5.220000	-403.8770	5.220000	27988.47
5.340000	1906.643	5.340000	30918.16
5.460000	6909.898	5.460000	38729.76
5.580000	8255.736	5.580000	17834.63
5.700000	6907.107	5.700000	-8653.294
5.820000	14599.11	5.820000	28207.81
5.940000	16075.41	5.940000	29423.95
6.060000	4580.446	6.060000	-29775.31
6.180000	-2501.472	6.180000	-46553.45
6.299990	-3046.579	6.299990	-32686.68
6.419990	1007.863	6.419990	-7771.345
6.539990	4450.337	6.539990	5449.699
6.659990	-1895.174	6.659990	-35164.12
6.779990	-4134.870	6.779990	-42226.15
6.899990	592.2988	6.899990	-10202.90
7.019990	-4900.276	7.019990	-33267.90
7.139990	-13168.97	7.139990	-53038.88
7.259990	-14155.02	7.259990	-31495.45
7.379990	-10175.60	7.379990	-3401.172
7.499990	-2037.099	7.499990	31961.83
7.619990	-2537.893	7.619990	16792.98
7.739990	-10365.33	7.739990	-23224.84
7.859990	-6663.691	7.859990	10102.76
7.979990	-212.9292	7.979990	42517.71
8.099990	-1417.545	8.099990	26730.40
8.219990	-1980.576	8.219990	21689.60
8.340000	-1527.583	8.340000	15827.63
8.460000	4144.204	8.460000	31344.69
8.580000	12648.72	8.580000	58115.68
8.700000	9013.509	8.700000	21346.57
8.820000	4134.388	8.820000	-3069.043
8.940000	8353.832	8.940000	24245.50
9.060000	9588.924	9.060000	20669.76
9.180000	8389.120	9.180000	9704.038
9.300000	7100.230	9.300000	-2779.436
9.420000	4991.131	9.420000	-18157.43
9.540000	9173.441	9.540000	2506.271
9.660000	9349.440	9.660000	-808.7243
9.780010	-84.61229	9.780010	-47302.98

INITIAL DISTRIBUTION LIST

		No. Copies
1.	Defense Technical Information Center Cameron Station Alexandria, Virginia 22304-6145	2
2.	Library, Code 0142 Naval Postgraduate School Monterey, California 93943-5002	2
3.	Professor Y. S. Shin, Code 69Sg Department of Mechanical Engineering Naval Postgraduate School Monterey, California 93943-5000	5
4.	Professor R. E. Newton, Code 69Ne Department of Mechanical Engineering Naval Postgraduate School Monterey, California 93943-5000	1
5.	Department Chairman, Code 69 Department of Mechanical Engineering Naval Postgraduate School Monterey, California 93943-5000	1
6.	Dr. N. T. Tsai Defense Nuclear Agency SPSS Washington, D.C. 20305-1000	3
7.	Dr. E. Sevin Defense Nuclear Agency Washington, D.C. 20305-1000	1
8.	Dr. M. L. Baron Weidlinger Associates 333 Seventh Avenue New York, NY 10001	1
9.	Dr. Ranlet Weidlinger Associates 333 Seventh Avenue New York, NY 10001	1

10. Dr. Andrew P. Misovec — 1
5202 W. Military Hwy
Chesapeake, Virginia 23321

11. Dr. B. Whang, Code 1750.2 — 1
Hull Group Head, Submarine Protection Div.
David Taylor Naval Ship Research
and Development Center
Bethesda, Maryland 20084

12. Dr. Huang, Code R14 — 1
Naval Surface Weapon Center
White Oaks
Silver Spring, Maryland 20910

13. LT G. F. DeConto — 2
47 Water Street
Sandwich, Massachusetts 02563

END

DTIC

6-86